INTRINSIC CONDUCTIVE POLYMER FOR RENEWABLE ENERGY APPLICATIONS

By

WAFAA ABOUSAMRA

A THESIS

Submitted in partial fulfilment of the requirements
for the degree of Master of Science in
Applied Chemistry Graduate Program of
Delaware State University

DOVER, DELAWARE
May 2017

This thesis is approved by the following members of the Final Oral Review Committee:

Dr. Young-Gi Kim, Committee Chairperson, Department of Chemistry, Delaware State University
Dr. Andrew Goudy, Committee Member, Department of Chemistry, Delaware State University
Dr. Cherese Winstead Casson, Committee Member, Department of Chemistry, Delaware State University
Dr. Amir Khan, External Committee Member, Department of Physics & Engineering, Delaware State University

To my parents, Zainab Yakout and Hussein Abousamra. Thank you for all the love you are giving me and for believing in me.

To my husband, Khaled Sadek. Thank you for all your support to me. I could not make it without you.

To my brothers, Wael, Walid and my sister Hend. Thank you for encouraging me all the time.

To my daughters and my son Nada, Nuha and Kareem Sadek. Thank you for supporting me and being patient with me during this journey

To all my family, thank you for everything. I would be nothing without you.

ACNOWLEDGMENTS

Undertaking this Master degree has been a truly challenging and interesting experience for me. I would not have been possible to make it without the help and support from many people. First, I would like to express my special appreciation and thanks to my advisor Dr. Young-Gi Kim for his full support and encouragements during my research. Without his continuous advice and support on both of my research and academic study success would have not been achieved. I really appreciate his patience and tolerance. I also enjoy this experience working with Dr. Kim.

I would also like to thank my committee members, Dr. Andrew Goudy, Dr. Cherese Winstead Casson and Dr. Amir Khan for their professional advices and guidance on my research. I also sincerely thank the professors Dr. Peter DiMaria, Dr. Qiquan Wang, Dr. Bizenuh Workie, Dr. Dula Man, Dr. Daniela Radu and Dr. Mukta Hendi. I learned more than I anticipated from these courses.

I spent a lot of time on my experiment but I could not make it without help from our lab members, Dan Yang, Omar Melton and Shehu Isa. I really appreciate the help from Mr. Todd Campbell for FTIR and UV-Vis training as well as Mr. Gregory Hopkins for his support during my research.

I like to gratefully thank my family members for their understanding and support during my graduate studies. Thank you for always believing in me and encouraging me to follow my dreams.

ABSTRACT

Abousamra, Wafaa, M.S. Intrinsic Conductive Polymer for Renewable Energy Applications. (2017)

(Faculty Advisor: Dr. Young-Gi Kim)

The conjugated polymers provide us promising characteristics which make them good candidates for electronic devices such as supercapacitors and polymer solar cells. Polyaniline is one of the most promising polymers for the unique electrochemical properties, easy preparation and environmental stability. However, polyaniline has been found to be insoluble in organic solvents, which limits its use in the electronic device applications. The molecular interaction between the polymers is the main reason that causes the poor solubility. In order to understand the effect of molecular structure modification, a series of polyaniline was synthesized modifying the polymer backbone and changing the counter anion. For the modified backbone, fluorine and sulfonic group have been introduced to the backbone of polyaniline using hydrochloric acid as a dopant which was observed to improve the solubility. Poly(2-fluoroaniline) was found to be soluble in organic solvents including tetrahydrofuran (THF), dimethylsulfoxide (DMSO), dimethylforamide (DMF) and chloroform. For the counter anion modification, a broad range of dopants were selected from small dopants to highly bulk dopants. For the small dopants, hydrochloric acid and hydrofluoric acids were used for modifying the molecular attraction between the polymer molecules. Extensive study of pH impact on the polymer solubility was conducted using a wide range of pH conditions from 1 to 13, for which alkaline solution was observed to increase the solubility.

Increasing the intermolecular space between the chains by introducing a bulky counter anion will help loosen the tight stacking between the molecules which lead to improve the solubility. *p*-Toluene sulfonic acid and dodecyl benzene sulfonic acid have been used as a dopant to synthesize polyaniline. Dodecyl benzene sulfonic acid doped polyaniline was observed to improve not only the solubility but also the electric conductivity.

Film coating process was applied on several substrates including glass plates and flexible substrate, applying a broad coating techniques covering Doctor blade coating, drop casting and dip coating. The effect of solution secondary doping has been investigated in depth, testing dodecyl benzene sulfonic acid doped polyaniline along with several secondary dopants including *m*-cresol, *p*-toluene sulfonic acid and thymol. The doping method proved to reduce the surface resistant from 6 MΩ/□ to 1 KΩ/□ with *p*-toluene sulfonic acid.

A secondary film doping using *m*-cresol, thymol and *p*-toluene sulfonic acid was observed to increase the electrical conductivity dramatically and to reduce the surface resistance, for which the surface resistance was observed to be changed from 6 MΩ/□ to 650 Ω/□ when *p*-toluene sulfonic acid was used. In order to elucidate the properties of the polymers, several instruments have been used.

TABLE OF CONTENTS

Page

LIST OF FIGURES

LIST OF ABBRIVIATIONS

APS	Ammonium peroxydisulfate
BuEt	Butoxy Ethanol
CB	Conductive band
CE	Counter electrode
CSA	Camphor sulfonic acid
D-A	Donor-Acceptor
DBSA	Dodecyl benzene sulfonic acid
DCE	1, 2 Dichloroethane
DMF	Dimethyl formamide
DMSO	Dimethyl sulfoxide
DNNDSA	Dinonyl naphthalene disulfonic acid
DNNSA	Dinonyl naphthalene sulfonic acid
EAPs	Electroactive polymers
EB	Emeraldine base
EDLC	Electrochemical double layer capacitors
EIA	Energy information administration
EQE	External quantum efficiency
ES	Emeraldine salt
ESCs	Electrochemical supercapacitors
ETL	Electron transporting layer
FTIR	Fourier transform infrared spectroscopy

^{1}HNMR	Proton nuclear magnetic resonance
HOMO	Highest occupied molecular orbital
HTL	Hole transporting layer
ICPs	Intrinsically conductive polymers
LEB	Leucoemeraldine base
LUMO	lower unoccupied molecular orbital
NMP	N, methyl-2-pyrrolidine
PA	Polyaniline
PCE	Power conversion efficiency
PFA	Poly(2-fluoroaniline)
PGA	Pernigraniline
PSCs	Polymer solar cells
p-TSA	Para-toluene sulfonic acid
RE	Reference electrode
SR	Surface resistance
THF	Tetrahydrofuran
VB	Valence band
WE	Working electrode

CHAPTER 1

INTRODUCTION

1.1 Aim:

In modern society, since the industrial revolution in the 19th century, all kind of activities including manufacturing, transportation, communication and military rely on energy.[1, 2] It is noticeable that the world population grows rapidly with a large contribution of this growth coming from the developing countries. Correspondingly, the demand on the energy has increased rapidly in the past couple of decades and it has been expected to keep increasing according to the statistics data that was provided by Energy Information Administration (EIA) as shown in **Figure 1**.[1- 5]

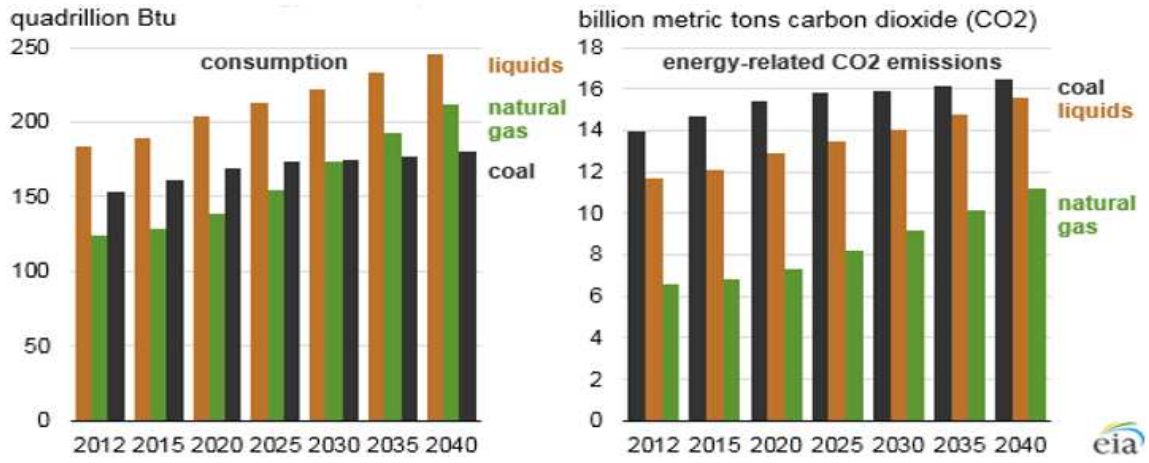

Figure 1: World Fossil Fuel Energy Consumption and Energy Related CO_2 Emissions (2012-2040).[4]

Fossil fuels including coal, oil and gas were reported to be the main source of energy consumed worldwide to produce electricity as shown in **Figure 2.**[5, 6]

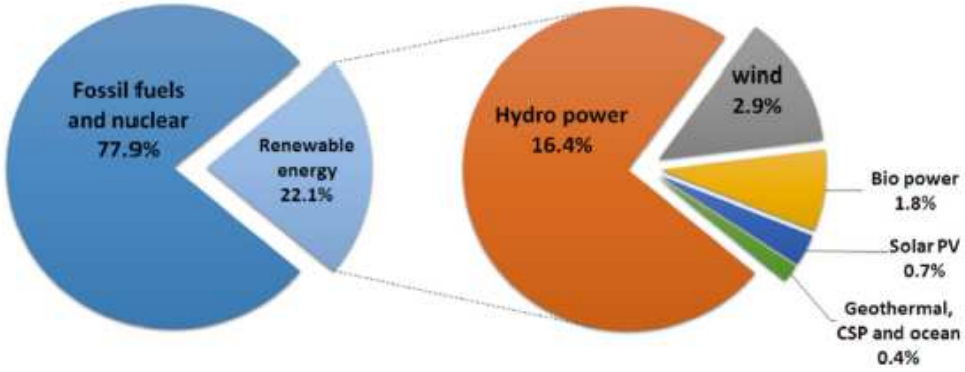

Figure 2: Global Electricity Production, 2013.[5]

However, the fossil fuels, as main source of energy, have several issues including pollution and sustainability of resource.[5,6] The environmental protection issue became a major issue concerning the emission of CO_2 gas which causes air pollution and leads to climate change due to the greenhouse effect.[5] **Figure 1** showed the CO_2 emission increasing since 2012 and how much expected to be by 2040.[5] The change of the climate was known to influence on the ecosystems. The realities of climate change and environmental pollution have made the scientists realize that we need to look for alternative energy solutions since the natural resources are expected to be depleted rapidly.[1- 3, 5- 7]

To find alternative source, the use of eco-friendly renewable energy is essential. The representative energy solutions include solar energy, wind energy, hydropower, biomass and biofuel.[5] **Figure 2** illustrates available renewable energy options.[5- 7] Solar energy recently attracted much attention for its availability and environmental safety, therefore it showed a significant growth compared to the other renewable sources as seen in **Figure 3**.[5- 7]

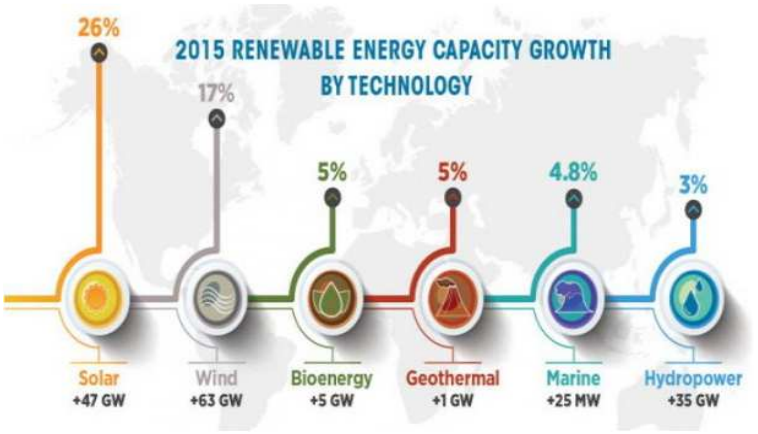

Figure 3: Renewable Energy Capacity Growth by Technology (2015).[8]

1.2 Polymers:

1.2.1 Definition:

The term polymer is derived from the word poly and the word mer in Greek, which mean many and parts, respectively. The term polymer denotes a long-chain molecule made up by repeating simpler unit called monomer.[9, 10] **Figure 4** shows how the polymer structured from the repeating units. It also has several common names including macromolecule since the polymer molecules have known to get high molecular weight.[9, 10] The monomers are held together to form polymer through covalent bonds, while the intermolecular forces or Van der Waals forces can attract the separate molecules together.[10] These bonds are playing a critical role in forming the polymer properties. Degree of polymerization is referred to the number of repeating units.[10]

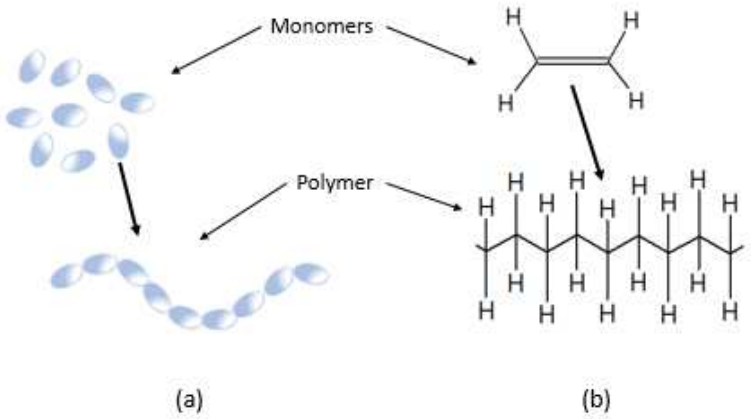

Figure 4: (a) Schematic Structure for Monomer and Polymer and (b) Chemical Structure for Polyethylene and The Monomer.

Polymers were known to show characteristic electrical and optical properties. Traditionally, the polymers were observed to exhibit insulating property because the molecules are poor in transporting charge along the molecular chain backbone.[11, 12] Typical examples of the polymers are introduced in the **Figure 5.**

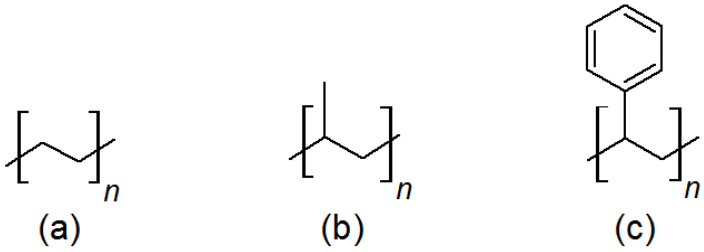

Figure 5: Chemical Structures for (a) Polyacetylene, (b) Polypropylene and (c) Polystyrene.

1.2.2 Classification:

Polymers have been classified into several families based on the structure, physical state, chemical structure and applications.[10] The polymer structure can be described as linear, branched or crosslinked. The polymer is classified to homopolymer where all monomers are identical or copolymer where two or more monomers are involved. **Figure 6** shows the structure types of the

polymers. Physical state is another way to classify the polymers that are crystalline, semi-crystalline and amorphous.[9, 10] When the crystalline polymers are arranged in crystal forms, the amorphous polymers have completely disordered arrangement.[9, 10] Application is one of the ways to classify polymer based on the end use for this polymer product.[9, 10]

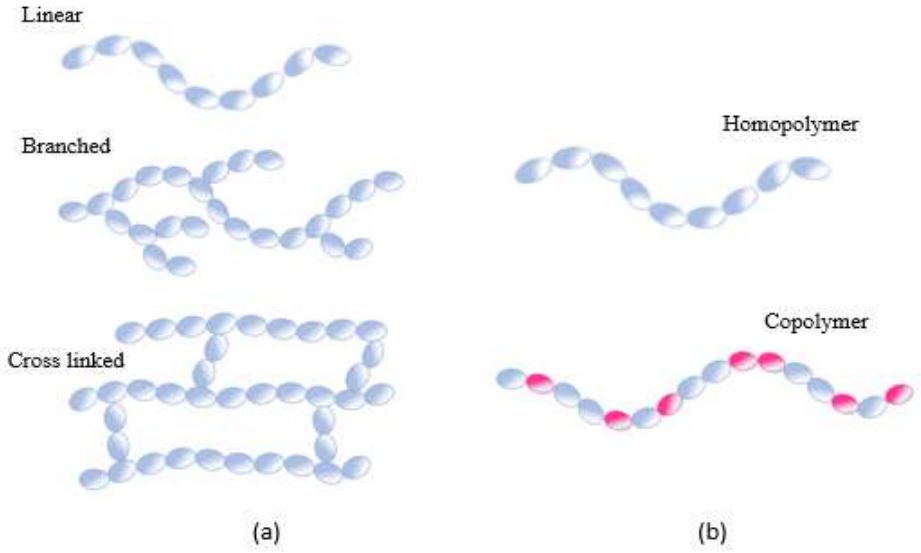

Figure 6: Schematic Structure (a) Linear, Branched and Cross Linked Polymer and (b) Homopolymer and Copolymer.

1.3 Intrinsically Conductive Polymers:

1.3.1 Background:

Intrinsically conductive polymers (ICPs) are a family of electroactive polymers (EAPs) that has been discovered in 1970th by Alan MacDiarmid, Alan Heeger and Hideki Shirakawa, separately.[9, 11-14] Electrical conductivity of polypyrrole and polyacetylene, shown in **Figure 7 (a** and **b)**, was discovered by these scientists and the discovery lead them to earn Noble prize in chemistry in 2000.[9, 11] The ICPs combine the properties of metal and plastic materials, exhibiting reversible redox behaviors and possessing electrical and optical properties of metals along with

additional distinctive characteristics of polymers including flexibility, low weight and good processability.[11, 15] These type of polymers are known as π-conjugated polymers and is commonly called synthetic metals. **Figure 7** presents some examples of the chemical structures of ICPs.

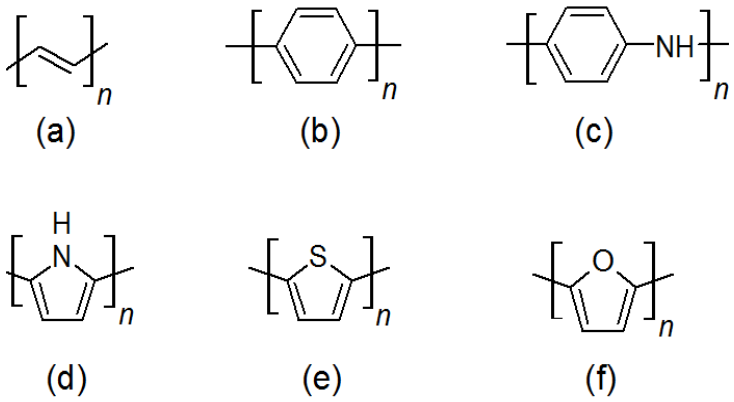

Figure 7: Chemical Structures for ICPs.

The properties of this type of polymers are the result of the unique structure, where single and double bond are placed alternatively along the polymer backbone which is called conjugation.[9, 12- 14] The conjugation structure allows the overlap of π-orbitals which are essential to delocalize the π- electrons on the polymer chain and to enhance electrical property as shown in **Figure 8**.[9, 12- 14]

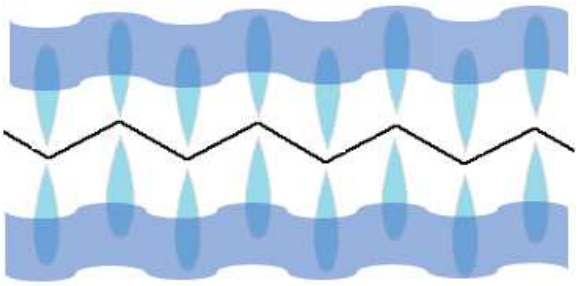

Figure 8: Illustration of Delocalization of π-Electron Over the ICP Chain.

Another characteristic for ICPs that allows it to conduct electricity is the low energy band gap.[16-18] The energy band gap for typical ICPs is known to be between 1 to 3 eV.[16] The band gap can be defined as the forbidden area for the electrons to be exist. With low energy band gap, the electrons in the valence band (VB) are able to be exited to the conduction band (CB) when the electrons absorb small amount of energy.[14] The energy band gap of the ICPs can be defined as the energy difference between the VB and the CB or energy difference between highest occupied energy level (HOMO) and lowest unoccupied energy level (LUMO).[14] **Figure 9** shows the HOMO and LUMO levels for ICPs as well as the band gap.

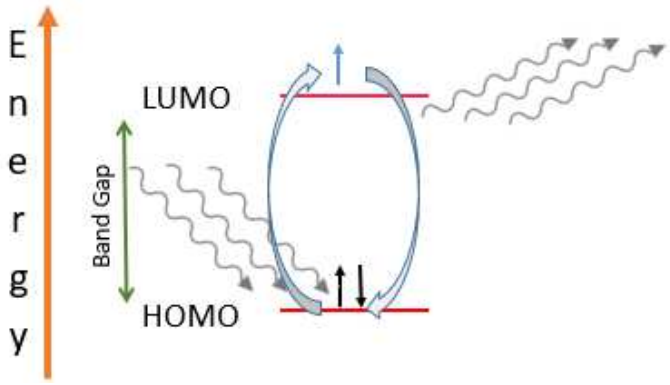

Figure 9: Schematic Diagram of HOMO, LUMO Levels and Band Gap for ICPs.

ICPs have attracted large numbers of academia and industrial research groups to explore the promising application opportunity in the field of electronics, coupling the characteristics of electronic and photonics properties.[11- 13]

1.3.2 Concept of Doping:

Neutral ICPs are known to be either insulator or semiconductor and exhibit very limited electrical conductivities.[11- 13] Doping is defined as a process removing electron from the valence band (p-doping or partial oxidation) or adding electron to the conduction band (n-doping or

partial reduction, which is far less common).[11, 19] The doping process can be accomplished by the addition of small quantity of donor or acceptor molecule that are chemical species called dopant or counter ion.[11, 13] Basically, the doping process is addition of electron to the conductive band to form n-doped or remove electron from the valence band to be p-doped. As a result of the doping, the electrical conductivity of ICP increased several fold to become highly conductive. The doping and dedoping are reversible processes without causing any mechanical or chemical degradation to the polymer.[11- 15] This doping process can be done chemically or electrochemically.[11- 13] The doping methods are shown in **Figure 10**.[11- 13]

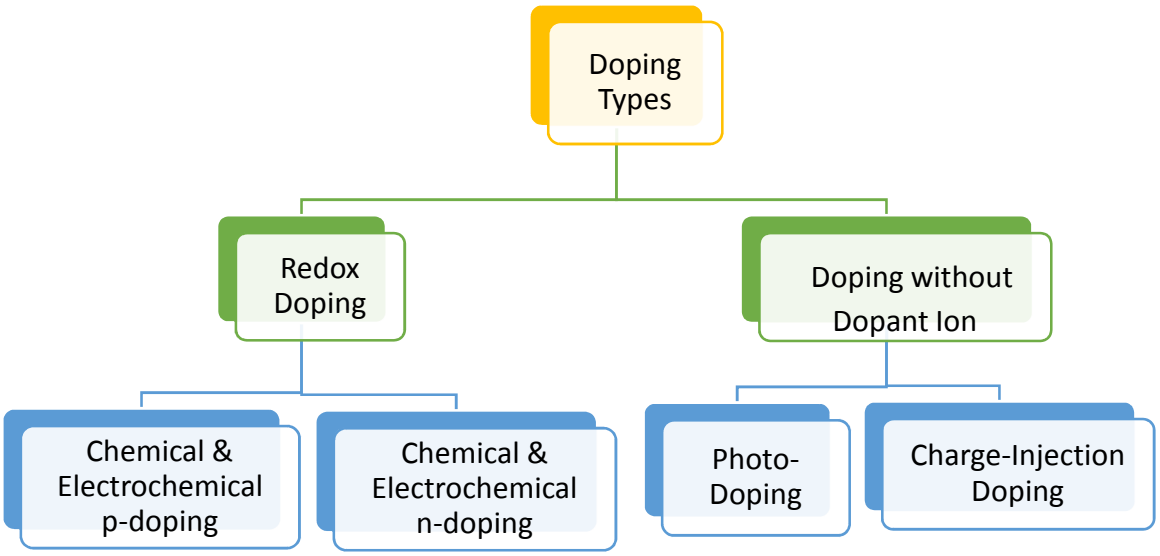

Figure 10: List of The Doping Types.

1.3.3 Electrical Conductivity:

Electrical conductivity can be defined as the ability of the matter to flow the electric current or charges through it.[11- 13] Doping (p or n) generates charge carriers which move in an electric field.[11- 13] Positive charges (holes) and negative charges (electrons) move to opposite

electrodes. This movement of charges is what actually responsible for electrical conductivity.[11-13] **Figure 11** shows the conductivity of ICPs compared to common materials and the effect of the doping level on the conductivity.

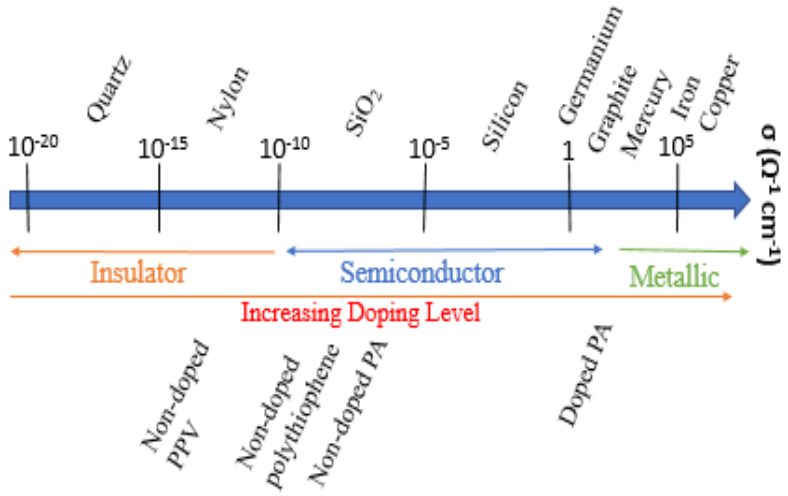

Figure 11: Conductivity of Some Polymers Compared to the Other Common Materials.

The electrical conductivity is reverse proportional to the resistivity as shown in **Equation 1**.[20] The resistivity can be defined as seen in **Equation 2**.

$$\sigma \propto 1/\rho \qquad \text{Equation 1}$$

$$\rho \propto RA/L \qquad \text{Equation 2}$$

Where σ is the conductivity (SI = Ω cm), ρ is the resistivity, R is the electrical resistance (Ω), A is the area of the cross section in the material and L is the length of the material piece.

1.3.4 Donor-Acceptor Polymer:

Donor-Acceptor (D-A) polymer defined as alternative copolymer that is constructed from two different units, electron donor and acceptor.[21-29] Donor units are usually thiophene or benzene having side group of alkoxy or alkyl group (p- type) while the acceptor units contain

aryl group with one or more electronegative atoms (n-type)**. Figure 12** shows some examples of D-A polymers chemical structures.[21- 29]

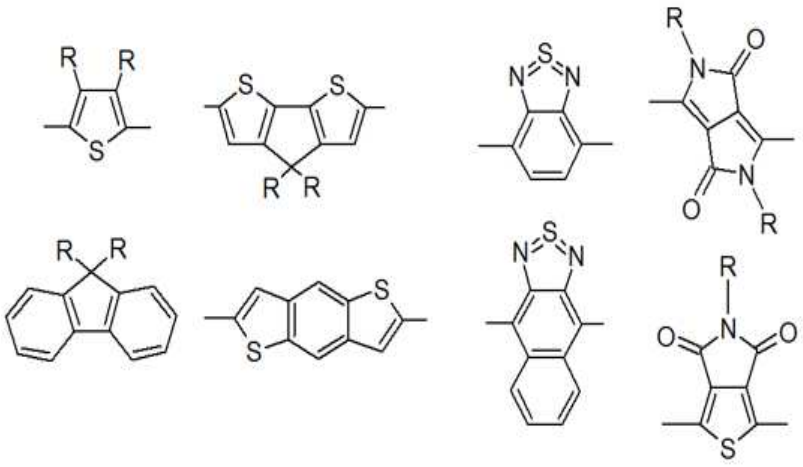

(a) (b)

Figure 12: Examples of Chemical Structures of (a) Donor Units, (b) Acceptor Units.

In order to synthesize the D-A conjugated polymers, Carbon-Carbon Cross-Coupling Reactions were used to achieve the desired structures.[30, 31] Still, Heck, Suzuki and Negishi are the most C-C coupling reactions that have been used for the synthesis using different organometallic compounds.[30, 31] Platinum, copper and Nickel have been used as metal catalysts in the cross-coupling reaction. The most common material of the catalyst is Palladium.[30, 31] The reaction mechanism goes through three basic steps. The first is oxidative addition of organohalide unit to the catalyst. The second step is the transmetallation step, this is when the second unit is attached.[30, 31] The last step is reductive elimination where the two units coupled to retrieve the catalyst. **Figure 13** shows a general schematic illustration for the C-C coupling reaction mechanism.

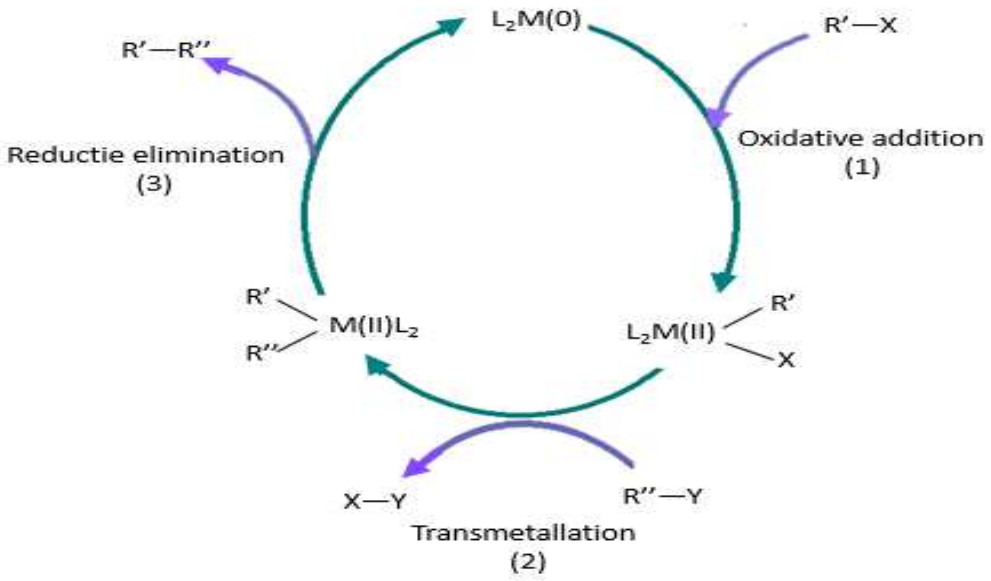

Figure 13: Schematic Diagram for General C-C Coupling Mechanism.

D-A polymer system is considered as the most common method to modify the energy band gap for the polymer.[32] New hybrid HOMO and LUMO levels were studied to form in the D-A polymer. The hybrid HOMO level is known to be higher than the HOMO level for the donor and the hybrid LUMO level is reported to be lower than the LUMO level for the acceptor unit.[32] **Figure 14** shows HUMO and LUMO levels of the D-A polymers. Consequently, the electrical conductivity of the polymer is modulated.

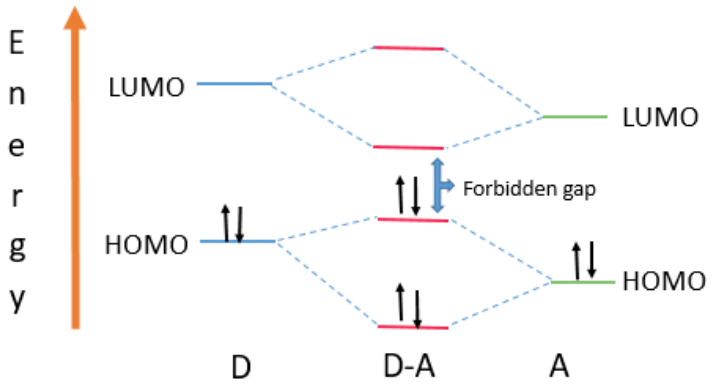

Figure 14: Schematic Diagram of the Hybrid HOMO and LUMO Levels for D-A Polymer.

1.3.5 Research Trend:

The optical and electrochemical properties of ICPs attracted a lot of attention from academia and industrial research groups in the past decades. Correspondingly, a large number of publications have been published, over 3000 article a year in the last decade in the area of ICPs as depicted in **Figure 15**.[32]

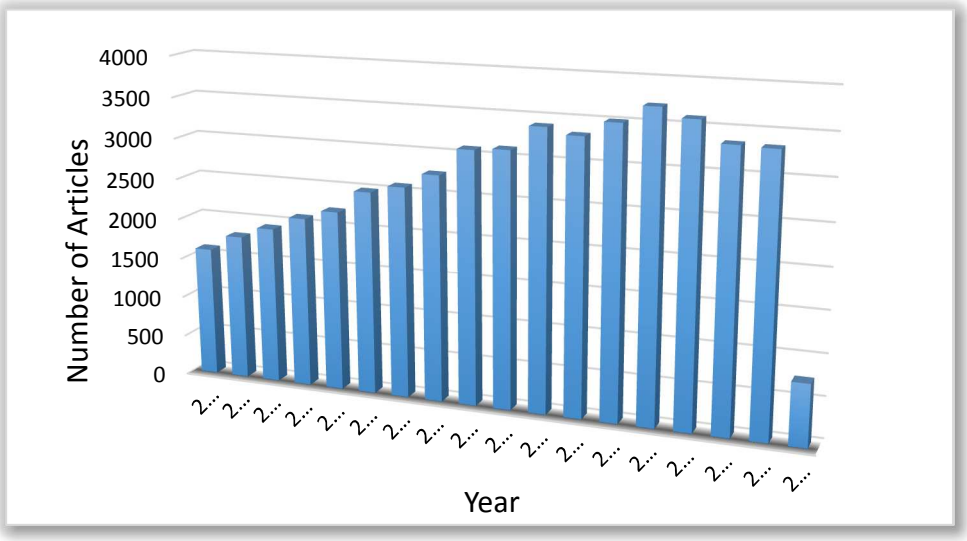

Figure 15: The Number of Articles Published on ICPs Over the Last Decade. Data Collected from Sci Finder Database.

1.4 Applications:

The optical and electrical properties of the conjugated polymers make them good candidates for several electrochemical applications.[11- 15] The potential applications for the ICPs system include energy production, energy storage, biomedical, sensors and filters as shown in **Figure 16**.[11- 15]

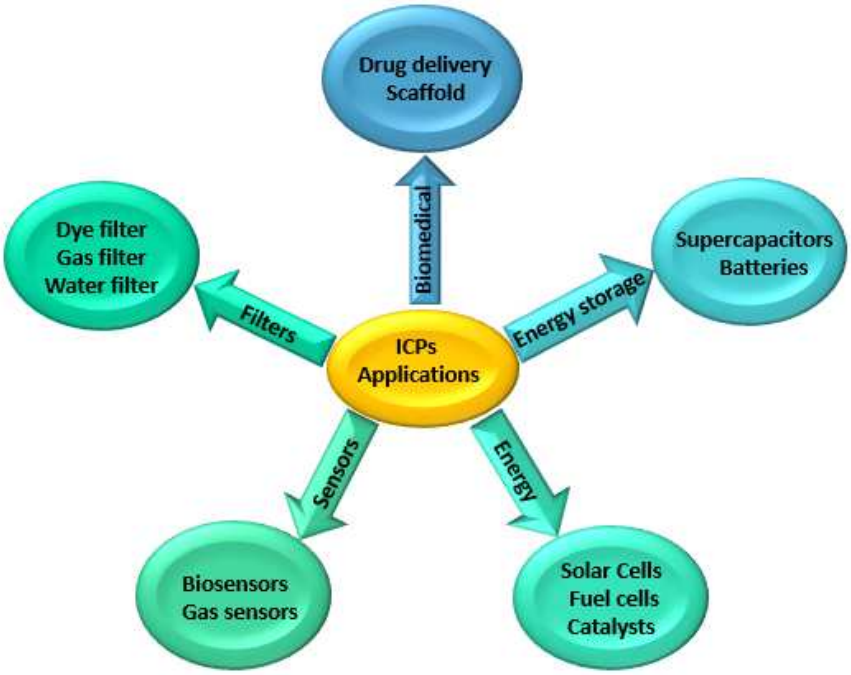

Figure 16: Scheme of ICPs Applications

1.4.1 Polymer Solar Cells:

Solar cells, that directly convert solar energy into electricity, are one of the most promising and efficient technologies to harvest solar energy.[33-35] Currently, the common solar cells, which are based on inorganic materials including crystalline silicon, cadmium telluride and gallium-arsenic, they exhibit efficiency from 20 to 41%.[4, 7, 36] Although the inorganic type solar cells have shown relatively high efficiency, they have been reported to have limitations including high cost processing, toxicity, lack of conformability and scarcity.[37] To overcome the limitations of the inorganic solar cells, scientists have developed polymer based solar cells. Polymer based solar cells (PSCs) harvest the solar energy using light harvesting polymers that have advantageous properties including low cost, flexibility, easy processability, environmental safety and low weight.[19, 19, 25, 28]

The polymer photovoltaic technology was built on the concept of photo induced electron transfer process between conjugated polymers and electron acceptors.[33] One of the representative conjugated polymers is D-A polymer which acts as electron donor polymer.[26] The driving force of photoinduced charge transfer through the conjugated D-A polymers and electron acceptors is the energy difference between the LUMO of the electron donor and the HOMO of the electron acceptor.[19, 26, 33] The external quantum efficiency (EQE) determines the ability of the polymer to convert photon to electron.[38] EQE equals to the ratio between the number of photons generated charges and the number of induced photons.[38]

Power conversion efficiency (PCE) is one of the major devices performance evaluation, has major factors including open circuit voltage (V_{oc}), short-circuit current density (J_{sc}), and fill factor (FF).[25, 33, 39-41] Thus, the overall PCE can be calculated following **Equation 3**.[40] Where P_{out} (in W/m^2) is the maximum electrical power output, P_{in} (in W/m^2) is the light intensity incident on to the device. V_{max} and J_{max} are the voltage and current at the maximum power point, respectively.

$$\text{PCE } (\eta) = P_{out}/P_{in} = \text{FF } (V_{oc}\, J_{sc})/\, P_{in} \qquad \text{Equation 3}$$

$$\text{FF} = (V_{max}\, J_{max}) / (V_{oc}\, J_{sc}) \qquad \text{Equation 4}$$

In the past few decades, scientists developed two different Types of PSCs that are conventional and inverted solar cells.[18, 33-42] PSCs include two electrodes (anode and cathode), hole transporting layer (HTL), electron transporting layer (ETL) and photo active layer. The only difference between the two PSCs is the layout of the layers as illustrated in **Figure 17**.[18, 33-42] The PSCs have been used to develop different structures including single-junction, bulk heterojunction, tandem and perovskite PSCs.[33-44] **Figure 18** shows examples of the structures.

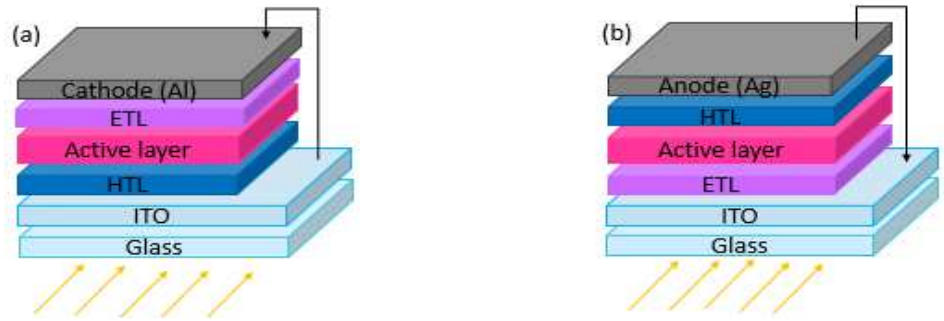

Figure 17: Structures of Polymer Solar Cells (a) Conventional and (b) Inverted.

PCE for bulk heterojunction and tandem PSCs were reported to exceed 9%, 11%, respectively.[34, 40, 42] The highest PCE was reported to be 20.1% for perovskite PSCs.[44]

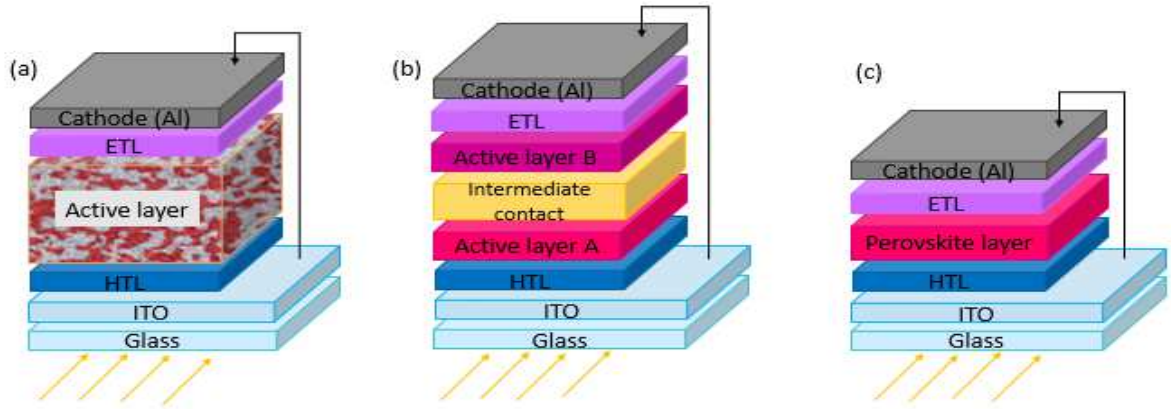

Figure 18: PSCs Structures (a) Bulk hetero-junction, (b) Tandem and (c) Perovskite.

1.4.2 Supercapacitors:

Supercapacitors are devices where energy is stored.[45-50] Electrochemical double layer capacitors (EDLC) or electrochemical supercapacitors (ESCs), pseudo capacitors and hybrid capacitors are examples of supercapacitors as indicated in **Figure 19**.[45-49] The fundamental difference between the ESCs and the battery is the form of stored energy.[45] The ESCs store energy in the form of electrochemical energy and the charge storage process is electrostatic non-faradic.[45-48] When applied voltage between the electrodes, an equal number of positive and

negative charges accumulate on the interface of the porous electrode.[45- 51] In this case, no electron transfer takes place across the electrode interface. In contrast, battery stores energy in the form of chemical energy which is faradic process and there is electron transfer across the electrode surface changing the oxidation state.[45-48]

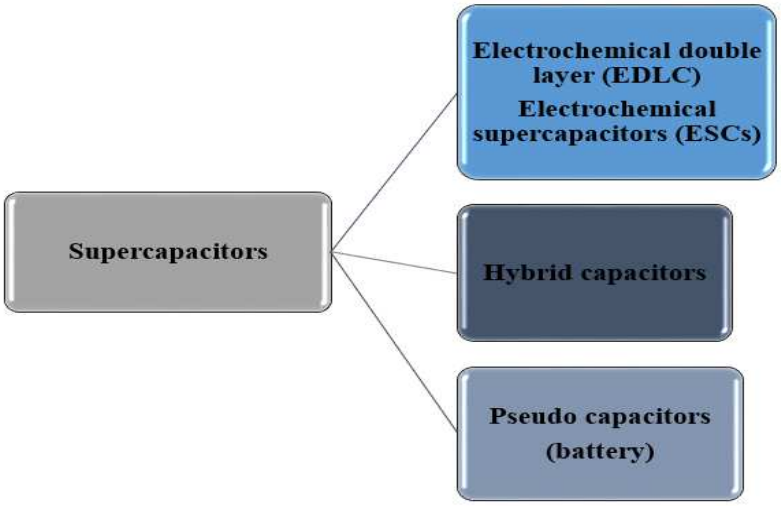

Figure 19: The Three Types of Supercapacitors.

ESCs are another area where ICPs can be used. The charge storing process in ICPs is beneficial in minimizing of the charge-discharge time and maximizing the cycle lives.[51-53] ESCs can also provide high specific power along with affordable specific energy.[52] Specific power, specific energy, specific capacitance and cycle-life are the main parameters to evaluate the device performance.[45, 53] While the specific power (W_s) is defined as the delivering rate of the energy per unit mass (W/Kg) gravimetrically, the power density (W_d) measured per unit volume (W/L) volumetrically.[45, 50] The specific energy is the amount of energy that can be stored per unit mass (Wh/Kg) or per unit volume to give the energy density which can be calculated from **Equation 5**.[45, 48, 50] The capacitance which is the ability to store energy, is calculated

gravimetrically (C_g) or volumetrically (C_v) as shown in **Equation 6**.[45, 50] I, E, Δt, m, v and ΔV are the current, energy, discharging time, mass, volume and the voltage, respectively. The capacitance of the electrode is proportional to the surface area and the pore size of the polymer.

$W_s = ½ C_g E^2$ or $W_d = ½ C_v E^2$ Equation 5

$C_g = I \Delta t/m \Delta V$ or $C_v = I \Delta t/v \Delta V$ Equation 6

ICPs based ESCs can be constructed using the same polymer or different polymers at the anode and the cathode electrodes.[45, 47, 53] Polyaniline and Polypyrrole are known to be suitable for positive electrode.[47] Polythiophene is reported to be used in both eledctrodes.[47] The ESCs can be classified based on the polymers according to oxidation and reduction states.[45, 47, 53] Type I and type III ESCs are symmetric using the same polymer at both electrodes while type II and type IV are asymmetric using different polymers.[45, 47, 53] Regarding the oxidation state, Type I and III the polymers that are p-doped at one electrode and are in neutral state in the other electrode when charged state.[45, 47, 53] Type II and IV use the polymers that are in p-doped at one electrode and are n-doped at the other electrode as presented in **Figure 20**.[45, 47, 53]

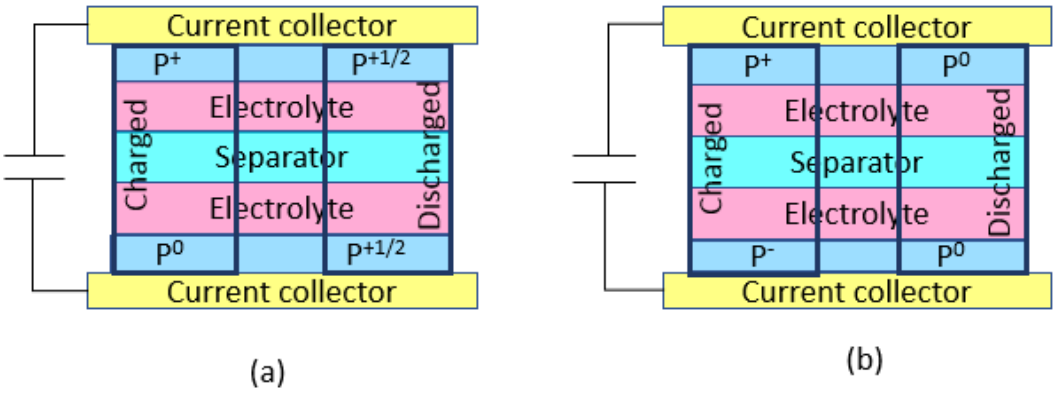

Figure 20: Schematic Configurations (a) Type I and III and (b) Types II and IV ESCs.

1.4.3 Biosensors:

Analytical biosensors are another field where conjugated polymers have been used for detection, quantification and monitoring of a variety of specific chemical species or analytes.[12, 54] The analytes could be chemical or biological component including metal, gas, virus, DNA or metabolism components.[55-57] The biosensors are constructed from two components, the biorecognition element or receptor and the transducer as illustrated in **Figure 21**.[12, 54] The receptor is usually impeded in between the analyte and the transducer.[12, 54] While the main job for the receptor is to activate the transducer using biochemical signal, the transducer converts and amplifies the biochemical signal to electronic output.[12, 54-57] Conducting polymer based biosensors belongs to the biosensor, where there is a direct binding of the receptor to a polymer which transduces and amplifies the optoelectronic signal.[12, 54-57] Two types of polymers are used in biosensors which are P-type polymer and n-type polymer. P-type polymer has been reported to show higher performance compared to n-type polymer.[12, 54]

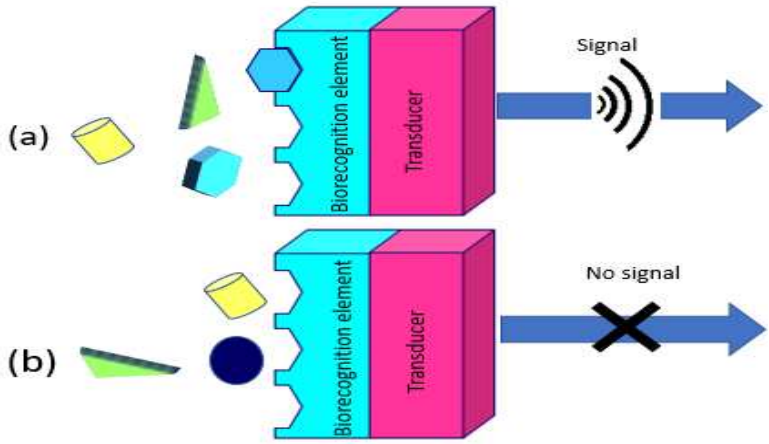

Figure 21: Schematic Diagram of Biosensor with (a) Target Analyte and (b) Nontarget Analyte.

There are four different types of biosensors including amperometric, potentiometric, conductometric and optical biosensors.[12, 54] The amperometric type detects the signal in the form of current that is produced from redox process at constant potential.[12, 54] Potentiometric type detects the potential changes.[12, 54] The conductometric type measures the change in the conductance and optical biosensors type builds on the idea of detecting the results of a biochemical reaction in the form of absorbance or emitting light.[12, 54]

Polymer based biosensors have wide range of applications including health care, environmental monitoring, food industry and immunochemistry fields.[12, 54]Recently, health care has been used biosensor extensively to detect several biocomponent including glucose, urea and cholesterol.[12, 54-57] Biosensors have potential to detect some gases for environmental purposes. The quality of the food in the industry can also be monitored using biosensors.[12, 54]

1.5 Research Objective:

The main objective of this research is summarized as synthesize ICPs having improved solubility and enhanced electrical conductive properties. The research was accomplished by completion of these specific aims:

1. Synthesis and characterization of polyaniline as one of the most promising ICPs
2. The study of intermolecular interaction of ICPs using different counter anions
3. The study of inter-relationship between structure and property of ICPs

CHAPTER 2

LITERATURE REVIEW

2.1 Background:

Among the intrinsically conducting polymers, polyaniline is one of the oldest and the most investigated. During the 19th century polyaniline has been synthesized from the aniline in the presence of potassium dichromate as the first synthetic dye in the British industry, Perkin's mauvein.[58] Previously polyaniline has been commonly named as "aniline black ", "emeraldine" or "nigraniline".[58-61]

2.2 Polyaniline:

Polyaniline was found to be one of the most promising ICPs owing to its low cost, easy to synthesize, tunable electrical conductivity, environmental stability.[62, 63] The properties of polyaniline attracted many researchers to consider the polyaniline in wide range of applications. The fact that polyaniline is able to switch from insulating form to conducting form opens the door for usage in electronic applications.

2.3 Structure:

Polyaniline exists in three chemical base forms based on the state of polymer oxidation.[59-65] The chemical structure of polyaniline contains two units, benzoid unit (reduced) which forms amine group on the nitrogen atom and quinoid unit (oxidized) which form imine group. [59-65] **Figure 22** shows the chemical structures in the three base forms and the salt form. While the fully reduced form of the polyaniline known as Leucoemeraldine base (LEB) (**a**), another form is the fully oxidized is known as Pernigraniline (PGA) (**b**). The last form is (**c**) Emeraldine base

(EB), contains the two units where X is the ratio between the oxidized and reduced units (0< X >1). [59-65] These three forms exhibit insulating property. Through doping process using counter anion, the previous three forms can be converted to conductive Emeraldine salt (**d**). The switch process between the base and the salt forms occur through a charge transfer or redox reactions in the polymer backbone. [59-65] Over the years, several counter anions have been explored including hydrochloric acid, sulfonic acid, camphorsulfonic acid, para toluene sulfonic acid and dodecylbenzene sulfonic acid.

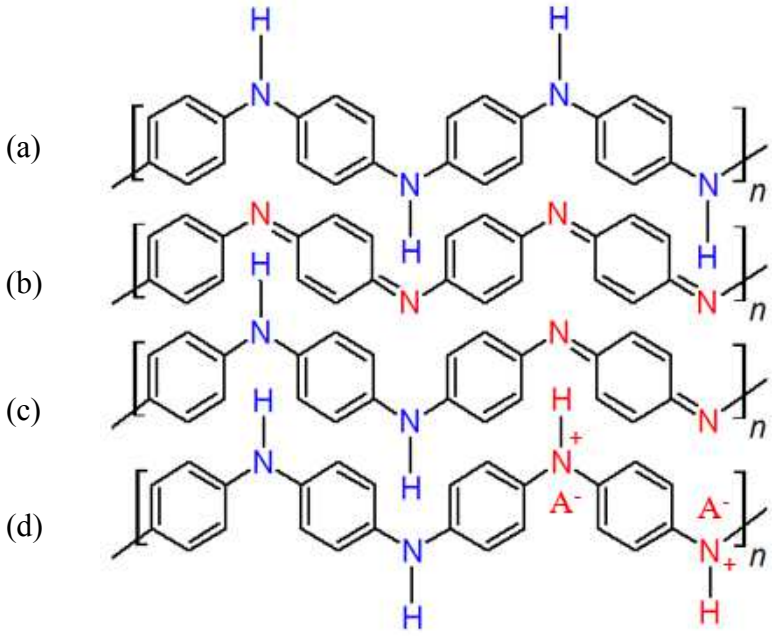

Figure 22: Chemical Structures of Polyaniline Base (a) Leucoemeraldine, (b) Pernigraniline, (c) Emeraldine base and (d) Emeraldine Salt.

2.4 Polaron and Bipolaron:

Polaron is a radical cation produced on the polymer backbone due to electron rearrangement when the polymer undergoes protonation process by dopant.[59, 60, 66] The protonation process leads to bipolaron formation on the imine unit.[59, 60, 66] Bipolaron form

undergoes electron rearrangement through internal redox reaction at the imine nitrogen by transfer an electron to quinoid unit nearby leading to formation of benzoid system.[59, 60, 66] This process leaves a single unpaired electron on each nitrogen atom which presents radical cation (polaron).[59, 60, 66] For the instability of the polaron radical cation, it starts to dissociate and delocalized freely on the polymer backbone forming two polarons.[59, 60, 66] The two process of polaron and bipolaron formation are illustrated in **Figure 23**. The polarons are the active centers for the conducting process and the polaron lattice is responsible for the conductivity of polyaniline.[59, 60, 66]

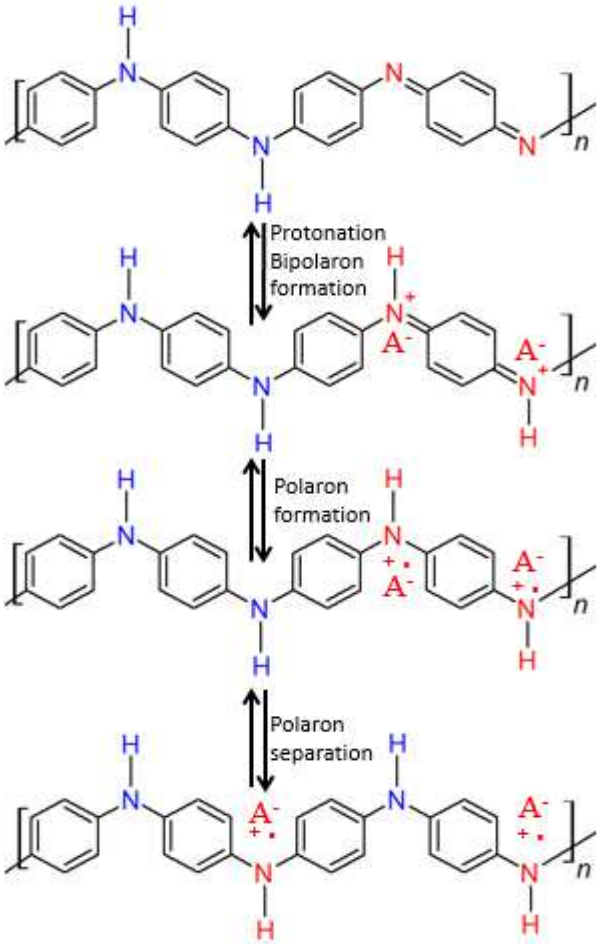

Figure 23: Polaron and Bipolaron Formation.

2.5 Synthesis:

In the past few decades, several methods have been proposed to synthesize polyaniline and its derivatives. However, all synthesis methods are classified into three main polymerization routes including electrochemical, chemical and catalytic polymerization as seen in the **Figure 24**.

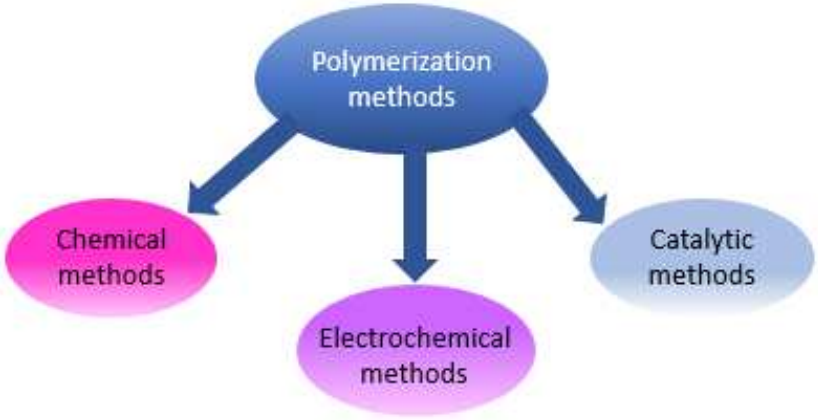

Figure 24: Polyaniline Polymerization Methods.

The mechanism of the polymerization is based on oxidation reaction and it is commonly called oxidative polymerization.[59-65] In this method, monomer aniline goes through an activation step where it is oxidized by initiator to form free radical cation.[45] There are several aniline radical cation forms based on its resonance of aniline as seen in **Figure 25**.[45]

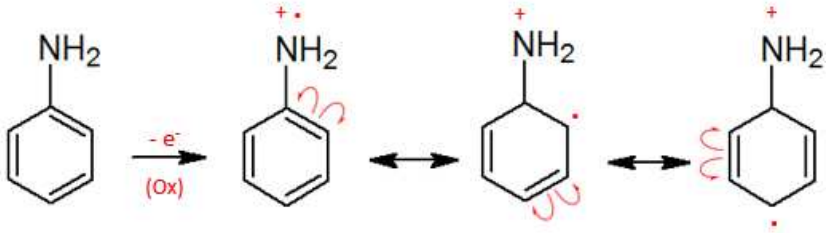

Figure 25: Resonance Forms of Aniline Radical Cation.

During the propagation step, the aniline radical cation interacts with another monomer aniline to be activated forming dimer and then trimer following the common polymerization

process.[45, 67] Similar to the monomer aniline, the oligomer needs to go through oxidation process in order to be activated and able to interact with monomers and to keep growing.[45, 67] The polymerization termination step is influenced by the concentration of oxidant and the monomer.[67] **Figure 26** depicts the suggested polymerization mechanism.

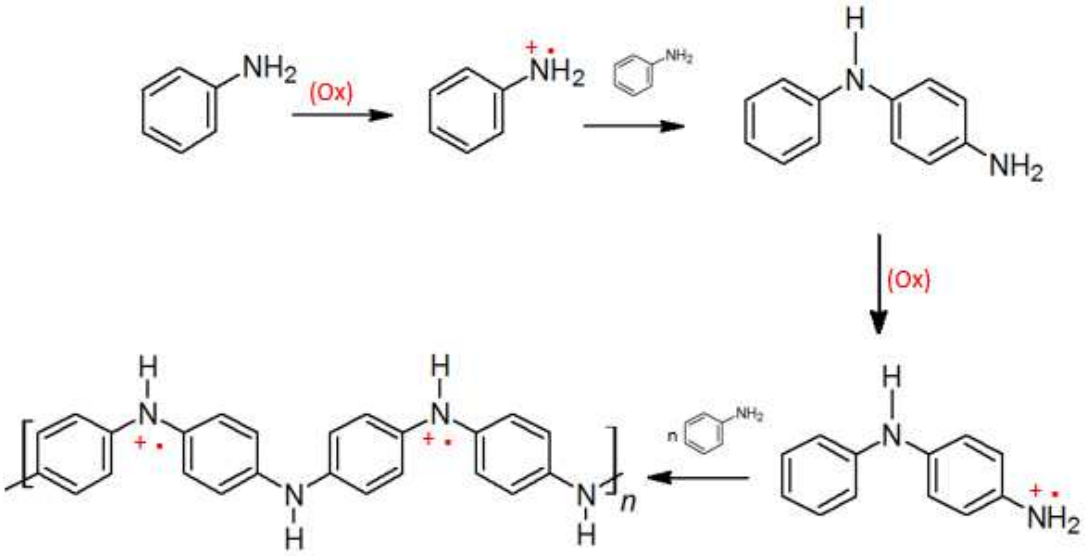

Figure 26: Mechanism of Oxidative Polymerization of Aniline.

2.5.1 Chemical Polymerization:

Chemical polymerization is considered to be the most common method for polyaniline preparation.[67,69, 70] Over the past decades, several chemical oxidants have been used for polymerizing aniline including ammonium peroxydisulfate ($(NH_4)_2S_2O_8$), potassium dichromate ($K_2Cr_2O_7$), ferric chloride ($FeCl_3$) and potassium permanganate ($KMnO_4$).[59, 60, 65- 72] The type of oxidant impacts the polymer yield as well as the electrical and physical properties of the polymer.[72] Ammonium peroxydisulfate (APS) and potassium dichromate (PDC) are proved to give higher yields, enhancing the polyaniline conductivity than the other oxidants.[71] The

chemical oxidation polymerization of aniline consumes a huge amount of oxidant, since the monomer activation relies mainly on the concentration of the oxidant.[67, 72] For the same reason, the ratio of the monomer and oxidant should be considered as an important factor during the synthesis.[67, 72] It is obvious that there is an inverse relationship between the ratio of monomer and oxidant and corresponding yields .[67, 72]

Several studies have been done to investigate polyaniline preparation. Hydrochloric acid, sulfonic acid, *p*-toluene sulfonic acid (*p*-TSA), dodecyl benzene sulfonic acid (DBSA), oxalic acid and phthalic acid are examples of the dopant that has been used.[59-66, 68-72]

The conventional chemical oxidative polymerization of polyaniline performed in an aqueous solution where aniline, oxidant and protonic acid are mixed. The mixture allows to react while maintaining low and constant reaction temperature (below 5 ^{O}C) for several hours.[59- 66, 72] For the fact that the polyaniline has poor solubility in water as well as in most organic solvents, after the polymerization, polyaniline precipitates are collected as a powder.[59- 66, 72] To overcome the solubility problem, another method has been developed using bulky organic acids as a dopant and surfactant including DBSA, dinonyl naphthalene sulfonic acid (DNNSA) and dinonyl naphthalene disulfonic acid (DNNDSA).[59- 66, 72] In this polymerization method, the reactants are mixed in aqueous solution forming emulsion (micelle) as seen in **Figure 27,** for that reason this method is called emulsion polymerization.[59- 66, 72] Although the product shows significant improvement, the polymer is not easy to separate from the mixture of the polymer solution which includes byproduct.[59- 66, 72]

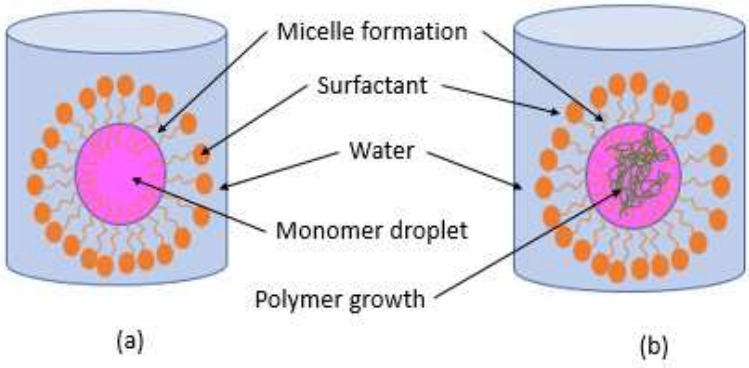

Figure 27: Scheme of Emulsion Polymerization.

Interfacial emulsion polymerization is another option to overcome the isolation problem.[59- 66, 72] Apart from the traditional chemical oxidative polymerization wherein all reactants are closely in contact inside aqueous solution, the reactants are mixed in heterogenous solvents.[59- 66, 72] Aniline monomers are dissolved in nonpolar solvents including chloroform while the oxidant in aqueous solution.[59- 66, 72] The polymerization process takes place in the interfacial surface between the aqueous and the organic layer**. Figure 28** illustrates polyaniline formation using the conventional chemical polymerization and the interfacial emulsion polymerization.[59- 66, 72]

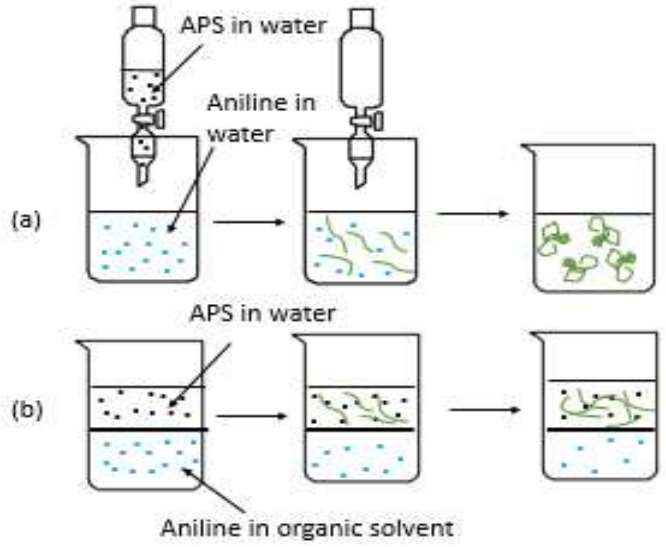

Figure 28: Schematic Diagram (a) Conventional Chemical polymerization, (b) Interfacial Emulsion Polymerization

2.5.2 Electrochemical Polymerization:

Electrochemical polymerization is used to prepare polyaniline by applying potential.[72] Although the chemical polymerization is the most common method to prepare polyaniline in a large scale, but on the other hand electrochemical polymerization can lead to polyaniline having high purity and controllable morphology.[72, 73] The purity of the polyaniline synthesized by electrochemical method is raised from eliminating the use of additional chemicals including oxidant and surfactant.[72, 73] Electrochemical method is also unique because the initiation and the termination steps is easily controllable applying potential which leads to control the film thickness.[72, 73]

The electrochemical cells use a working electrode (WE), a counter electrode (CE) and a reference electrode (RE). The electrodes are dipped in electrolyte solution containing monomer in water and dopant.[72, 73] General WE (cathode) material is platinum or carbon while CE (anode)

uses platinum, conductive glass or metal.[72, 73] To initiate the polymerization, a required potential applies between the working and the counter electrodes. The termination for the reaction can be done by stopping the potential. Controlling the applied potential time, the thickness of the polyaniline film can be controlled. Electrode materials, dopant, pH of the solution and the solvent strongly affect the polymerization process. **Figure 29** shows the basic electrochemical cell components and the polymerization process.

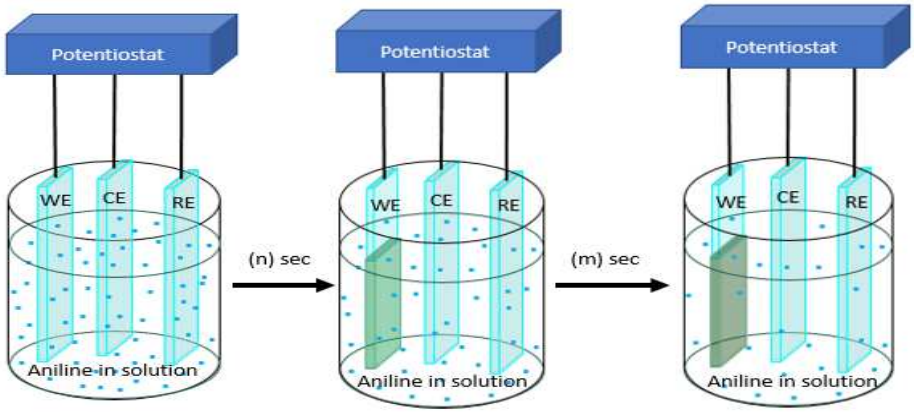

Figure 29: Schematic Diagram of Polyaniline Electrochemical Polymerization.

2.5.3 Catalytic Polymerization:

Catalytic polymerization is a green approach to synthesize a large-scale polyaniline where eco-friendly oxidant including hydrogen peroxide (H_2O_2) replaces the traditional chemical pollutant ones.[74, 75] The byproduct during H_2O_2 reduction process is water which it environmentally safe. [74, 75] Although this process is a slow process, it can be accelerated by using a metal catalyst. Several metals have been investigated to use as catalyst over the years including copper, gold, iron and palladium.[74, 75]

Copper promoted polymerization was reported for the first time in 1994 not only introducing the catalytic approach for polyaniline synthesis but also incorporating the usage of oxygen as green oxidant.[74, 75] Using simple copper salt including copper chloride and copper bromide, highly branched polyaniline base was synthesized showing insulating properties. To obtain a conductive polyaniline using this method, a more sophisticated copper salt is required.

2.6 The Factors Affecting Polyaniline Electrical Conductivity:

The electrical conductivity of polyaniline can be affected by several factors including, the molecular weight of the polyaniline chains, the type and the percentage of doping, the percentage of crystallinity, moisture level, the oxidation level and the molecular arrangement.[72, 76]

2.6.1 Molecular Weight:

The electrical conductivity of polyaniline depends on the molecular weight of the polymer chain or the number of repeating units.[72] A certain molecular weight is necessary for the polymer chain in order to be conductive.[72] Increasing the number of the repeating units of the polymer leads to long- range delocalization of the charge carriers through formation of conjugation. However, some distortions in the chain can be developed at very high molecular weight which has a negative impact on the polymer electrical conductivity. [72]

2.6.2 Type and Percentage of Doping:

Doping is considered be the second most important factor for achieving high level of conductivity.[72] As shown earlier, protonation by doping the polymer with acid forms the polarons. The protonation level plays a key role of the conductivity. There is a proportional relationship between the doping level and the conductivity. The structure of EB has alternative

benzoid and quinoid units which leads to the highest conductivity at 50 % doped. The nature of the dopant is proved to impact the conductivity of the polymer.[72]

2.6.3 Percentage of Crystallinity:

Generally, the internal structure between the polymer chains also affect the electrical property for the polymer. Increasing the crystallinity level leads to improve the electrical conductivity because of the increased order of the chains is essential for charge carrier mobility. EB is amorphous polymer and it is well known that the crystallinity level is increased by doping transforming to semi amorphous.[72]

2.6.4 Oxidation Level and Molecular Arrangement:

Among the polyaniline structures, only EB is able to form polarons where the current is carried out by holes in the presence of dopant.[72]

2.6.5 Moisture Level:

The moisture level is found to impact the conductivity of polyaniline. The conductive polyaniline was observed to be changed modifying the moist level during time. The conductivity of polymer shows improvement when the polymer has trace of water due to increase the charge delocalization along the backbone of the polymer.[76]

2.7 Applications:

In the past couple of decades, polyaniline has been introduced in several applications. The most important applications for polyaniline includes polymer solar cells, supercapacitors and sensors.

2.7.1 Polyaniline in Polymer Solar Cells:

Several research groups have attempted to use polyaniline as a HTL in PSCs. Poly (3,4 ethylenedioxythiophene): poly (styrene sulfonate) (PEDOT: PSS) is used as the most common HTL in PSCs.[77- 80] Sulfonated polyaniline doped with HCl has been utilized as HTL replacing the PEDOT: PSS for accommodating active layers including PBDTTT-C-T, PTB7, PBDTBDD, PBTTDPP-T, PDPP3T or P3HT.[77] **Figure 30** shows the chemical structures of the typical polymers used as the active layer. Polyaniline as HTL is found to be very effective for improving the overall performance of PSCs.[77] PCE for PSCs using polyaniline was reported to approximately 9% using PBDTTT-EFT as an active layer even with limited thickness of polyaniline (1.3 nm).[77] Polyaniline does not only prove to show improvement of the PCE but also does show enhancement of environmental stability.[78] Study has been done using polyaniline doped with camphorsulfonic acid (CSA) replacing PEDOT: PSS using P3HT: PCBM as active layer.[78] In this work, the PEDOT: PSS-based cells exhibits fast degradation, while PA: CSA exhibits more stable performance over two years.[78]

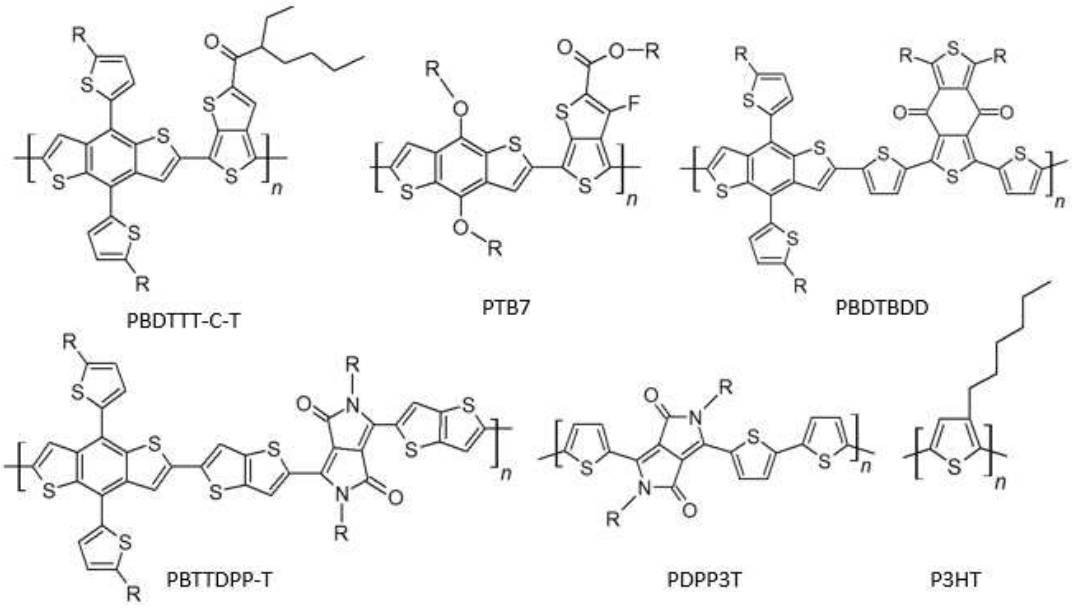

Figure 30: Chemical Structure of Typical Examples of Active Layer Polymers.

Recently, several metal oxides have been used to form hybrid materials and nanocomposites with polyaniline including titanium dioxide (TiO_2) and silica (SiO_2).[79, 80] Investigating the hybrid polyaniline/ TiO_2 shows high crystalline nature of the film and homogeneous distribution of TiO_2 in the polymer improving the charge transportation.[79] In addition, the hybrid material enhances the optical absorbance which effectively enhances the performance of the PSCs.[79] Utilizing SiO_2 with polyaniline as HTL in PSCs instead of using the conventional PEDOT:PSS exhibits enhancement in the fill factor.[80] Both study confirms that the hybrid nanoparticles with polyaniline are a promising HTL candidate as an alternative of PEDOT:PSS in PSCs.[79, 80]

2.7.2 Polyaniline in Supercapacitors:

Polyaniline is considered to be one of the most promising electrode material due to its high theoretical specific capacitance of ~ 3400 F/g as well as fast redox reversibility.[81, 82] However,

the polymer exhibits limited mechanical and cycling stability for which, several composites of polyaniline have been investigated in order to improve the mechanical and cycle stability.[81,82] Carbon nanotube, graphene, graphene oxide and molybdenum disulfide are the typical examples of the composite material that has been used with polyaniline.[81- 88] Composites of polyaniline with carbon nanotube were reported to be able to provide enhanced specific capacitance as high as 531F/g.[83] Polyaniline in this study were prepared through electrochemical polymerization in the form of nanofiber on a substrate of carbon paper.[83] In another work, carbon nanotube composites showed good volumetric capacitance of 40.5 F/cm^3 using nanoribbon structured polyaniline that was deposited on cellulose fiber (Kim wipe).[84] This composites exhibit not only a good electrochemical performance but also mechanical and durability and flexability.[81- 84]

Three dimensional macroporous graphene/polyaniline composites have been investigated by several research groups.[85, 86] Graphene/ polyaniline composites were observed to have specific capacitance up to 1295 F/g.[95] The capacitive retention for this type of composites was recorded to be 69% after 5000 cycles.[86] It has been reported that the graphene oxide/ polyaniline composites were reported to exceed the specific capacitance of 1145 F/g.[87, 88] Some other groups have explored polyaniline with carbon nanotube and graphene array which were reported to have specific capacitance of 987 F/g.[89] Molybdenum disulfide/reduced graphene oxide/ polyaniline composites were resulted in outstanding energy storage performance in terms of capacitive property that was reached to 1224 F g−1.[81] Polyaniline deposited on cobalt-based metal-organic framework on carbon cloth was observed to show an extraordinary capacitance.[90]

2.7.3 Polyaniline in Sensors:

Sensors are another area where polyaniline has been used standing by itself or incorporated in composites including titanium dioxide, gold, iron oxides and reduced graphene oxides.[91- 24] One of the typical examples is dodecyl benzene sulfonic acid doped polyaniline. This outstanding polyaniline was reported to be used for gas sensor using spin coated method to prepare thin film for quantitative detection of ammonia (NH_3) under ambient conditions (27 ^{o}C).[91]

The composite of polyaniline and materials are promising in constructing sensors. The size and the morphology of nanoparticle in the composites play a critical role in the sensitivity. The sensitivity of gold nanostars/polyaniline composites (average size of nanostars ∼170 nm) has been investigated toward ammonia gas. It was reported that the sensitivity of the composite increase by 52%, that is superior to 7% value for pure polyaniline.[92] Moreover, the gold nanostar−polyaniline composites showed a fast response time as short as 15 sec at room temperature.[92] Polyaniline nanofiber and iron oxide–reduced graphene oxide were also used in hydroquinone sensors and the composites showed high limitation of detection.[93]

One of the representative applications of polyaniline composites in sensors is biosensors.[94] Gold nanoparticles and polyaniline- titanium dioxide nanotube composites was reported to enhance the sensitivity of biosensor for detecting lactase.[94]

CHAPTER 3

EXPERIMENTAL

3.1 Materials

Aniline, 2-fluoroaniline (99%), acetone (100%), dodecyl benzene sulfonic acid (DBSA), hydrofluoric acid, chlorosulfonic acid (97%) (CSA), 2-butoxyethanol (99%) (BuEt), *o*-xylene (99%), *m*-cresol (99%), thymol (99%), *p*-Toluene sulfonic acid monohydrate (*p*-TSA), tetrahydrofuran (99%) (THF), N- methyl-2-pyrrolidone(NMP) and N, N dimethyl formamide (DMF) were obtained from ACROS chemical company. Ammonium peroxydisulfate (APS), hydrochloric acid (12N), sulfonic acid, dimethyl sulfoxide (DMSO) and the glass plates were purchased from Fisher Scientific company. 1, 2 Dichloroethane (99%) (DCE) was ordered from Alfa Aesar company. Chloroform-D1 (99.8%) was obtained from MagniSolve company. Silver paint was obtained from TED PELLA company. All the materials were used without further purification.

3.2 Synthesis of Polymers

In early stage of the research, several polyanilines were synthesized modifying the polymer backbone using small counter anions. The research moved ahead using bulkier counter anion than before to synthesis soluble polyaniline.

3.2.1 Polyaniline Using Small Dopant (PA.Cl), (PA.F):

In this experiment, polyaniline was prepared by chemical oxidative polymerization following A. G. MacDiarmid method.[59- 62] Two different small size acids, hydrochloric acid and hydrofluoric acid were used as counter anions (dopants).[59--62] In a round bottom flask, 0.0504

moles of APS were dissolved in 200 ml of 1 M acid. In another flask, 0.2190 moles of aniline were dissolved in 300 ml of 1 M acid (below 5 ^{O}C). The molar ratio between the monomer: oxidant was kept 4:1. APS solution was added to aniline solution over 1 min and let the reaction run for 1.5 h under constant stirring speed keeping the temperature below 5 ^{O}C. Blue-green color was observed after 30 mins indicating that polyaniline was started to form. Partially doped (about 42%) polymer precipitates were collected using Buchner vacuum filtration (7.5 cm diameter) after reaction. The precipitates were washed at a portion of 60 ml using 500 ml of 1 M acid, maintaining the liquid level above the precipitate to avoid cracking then kept under suction for 10 min until partially dried. Half of the moist precipitates were kept for drying process. In order to maximize the doping level, the other half of the moist precipitates were treated with 500 ml of 1 M protonic acid under constant stirring speed at room temperature for 15 hours. Fully doped polymer was collected and washed. The filtered polymer was dried following the same procedure that is mentioned earlier. Partially dried powder of polyaniline and partially and fully doped polyaniline were then dried in the dynamic vacuum for 48 hours and then kept sealed at room temperature.

3.2.2 Polyaniline with Modified Backbone:

3.2.2.1 Fluorinated Polyaniline with HCl (PFA.Cl):

The same A. J. MacDiarmid method was used to synthesize fluorinated polyaniline starting the reaction with monomer 2-fluoroaniline monomer.[59- 62, 95] In a round bottom flask, 0.0504 moles of APS was dissolved in 200 ml of 1 M HCl. In another flask, 0.2190 moles of 2-fluoroaniline was dissolved in 300 ml of 1 M HCl below 5 ^{O}C. The molar ratio between the

monomer and oxidant was kept 4:1. APS solution was added to aniline solution over 1 min and let the reaction run for 1.5 h under the constant stirring speed keeping the temperature below 5 ^{O}C. Yellow color was appeared after 30 mins and then started to become dark brown, indicating that poly(2-fluoroaniline) was formed. Partially doped (about 42%) polymer precipitates were collected using Buchner vacuum filtration (7.5 cm diameter). The precipitates were washed in a portion of 60 ml using 500 ml of 1 M HCl maintaining the washing liquid level above the precipitates to avoid cracking and then kept under suction for 10 min until partially dried. Half of the moist precipitates were kept for drying process. In order to maximize the doping level, the other half portion of the moist precipitates were treated using 500 ml of 1 M HCl under the constant stirring speed at room temperature for 15 hours. Fully doped polymer was collected and washed. The poly(2-fluoroaniline) was dried following the same procedure that is mentioned earlier. Partially dried polymer powder and partially and fully doped polymer were additionally dried in the dynamic vacuum for 48 hours then kept sealed at room temperature.

3.2.2.2 Partially Fluorinated Polyaniline with HCl (PFA.PA.Cl):

Partially fluorinated polyaniline was prepared following the same procedure for polyaniline and fluorinated polyaniline was synthesized mixing of aniline and 2-fluoroaniline monomer at a mole of 50% and 50%.[59- 62, 95] In a round bottom flask, 0.0504 moles of APS dissolved in 200 ml of 1 M HCl. In another flask, 0.1095 moles of aniline and 0.1095 moles of 2-fluoroaniline were dissolved in 300 ml of 1 M HCl below 5 ^{O}C. The molar ratio between the monomer and oxidant was kept 4:1. APS solution was added to the monomer solution over 1 min and let the reaction run for 6 hours under the constant stirring speed keeping the temperature below 5 ^{O}C. Yellow color was appeared after 30 mins and then the color was observed to be

changed to blue green. The polymer precipitates were collected using Buchner vacuum filtration (7.5 cm diameter). The precipitates were washed in a portion of 60 ml using with 500 ml of 1 M HCl maintaining the liquid level above the precipitate to avoid cracking then kept under suction for 10 min until partially dried. Partially dried polymer powder was dried in the dynamic vacuum for 48 hours and then kept sealed at room temperature. **Figure 31** illustrates previous experimental set up.

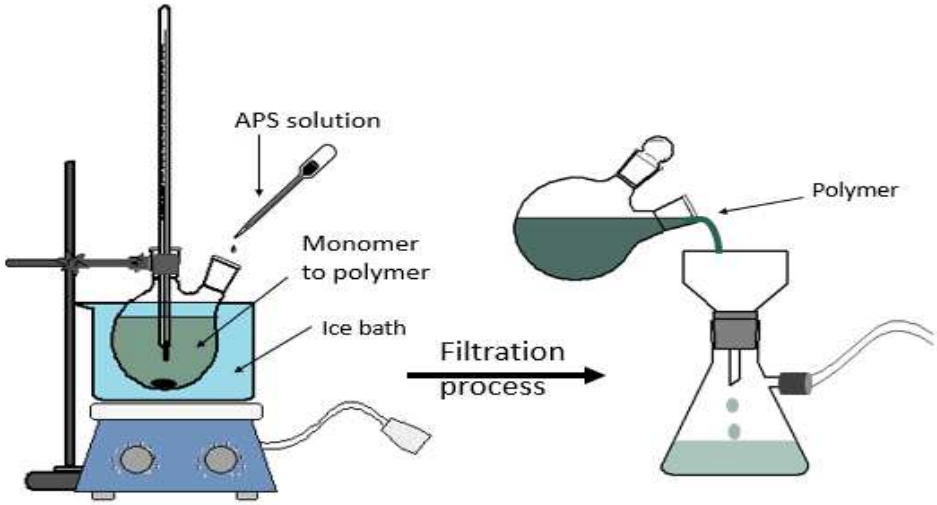

Figure 31: PA.Cl and PFA.Cl Experimental Set Up.

3.2.2.3 Sulfonated Polyaniline with HCl (PSA.Cl):

Sulfonated polyaniline (PSA.Cl) was prepared using the polymerization method of polyaniline salt (PA.Cl) previously prepared.[96] In a flask, 0.5 g of polyaniline salt was dispersed in 15.5 ml of boiling DCE at 80 ^{O}C. 1.2 g of CSA diluted with 1.1 ml DCE in another flask was added to PA.Cl solution dropwise over 30 mins. The reaction was held for 5 hours. Chloro-sulfonated polyaniline was precipitated and filtered using Buchner vacuum filtration (7.5 cm diameter). 28 ml of deionized water added to the precipitates in a flask and let a hydrolysis

reaction run for 3 hours then the precipitates filtered and washed using and 40 ml of acetone. Wet cake was dried in dynamic vacuum for 24 hours. The chemical reactions for the previous polyaniline synthesis are illustrated in **Figure 32**.

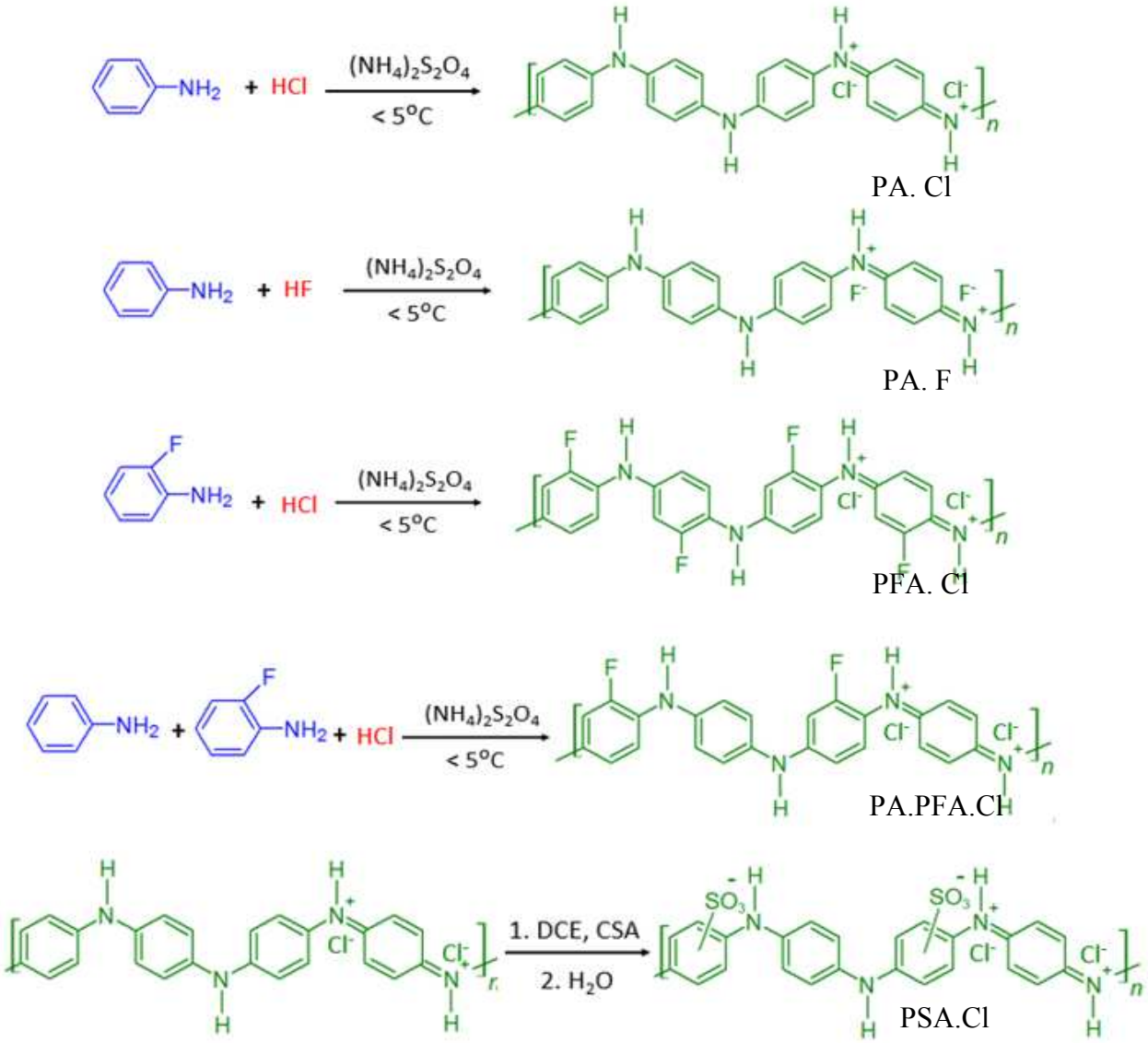

Figure 32: Chemical Reactions of Polyaniline Synthesis.

3.2.3 Polyaniline with Bulky Dopant:

3.2.3.1 Polyaniline doped with *P*ara-Toluene Sulfonic Acid (PTPA):

Polyaniline doped with *p*-TSA was synthesized using emulsion polymerization method.[68] An aqueous solution prepared by dissolving 14.7 g of *p*-TSA and 27 g of BuEt in 125 g of DI water under continuous stirring speed then cooled down to 5 ^{O}C. 6 g of the monomer (aniline or 2- Fluoroaniline) was added to the dopant solution at low temperature. APS solution was prepared by dissolving 17.64 g of APS in 37 g of DI water. APS solution was added to *p*-TSA and monomer solution dropwise over 30 mins. The reaction was held for 8 hours under stirring below 5 ^{O}C. The precipitates were collected using Buchner vacuum filtration (7.5 cm diameter). The precipitates were washed at a portion of 15 ml using 60 ml DI water maintaining the liquid level above the precipitates to avoid cracking and then kept under suction for 10 min until partially dried. The partially dried precipitates were kept under dynamic vacuum for 48 hours till fully dried and then stored at room temperature.

3.2.3.2 Polyaniline with Dodecyl Benzene Sulfonic Acid (DBPA):

The same procedure for PTPA preparation has been used for DBPA.[68] Polyaniline doped with DBSA was synthesized by preparing a solution containing 25.24 g of DBSA, 27 g of BuEt and 125 g of DI water under continuous stirring speed and then cooled down to 5 ^{O}C. 6 g of the monomer (aniline or 2- Fluoroaniline) was added to the dopant solution under low temperature. APS solution was prepared by dissolving 17.64 g of APS in 37 g of DI water. APS solution was added to DBSA and aniline solution dropwise over 30 mins. The reaction held for 8 hours under stirring speed keeping the temperature below 5 ^{O}C. 200 g of xylene was added to collect polymer in the organic phase and then the water was discharged after the separation observed. Washing

the solution prepared using 0.07 g of sulfuric acid and 68.4 ml of DI water then the aqueous solution was discharged to get rid of APS and monomer. The final washing was done by adding 70 ml of DI water only then discharged the aqueous layer a couple of times. **Figure 33** shows the experimental set up for the PTPA and DBPA synthesis. The chemical reaction for the bulky dopant base polyaniline are shown in **Figure 34**.

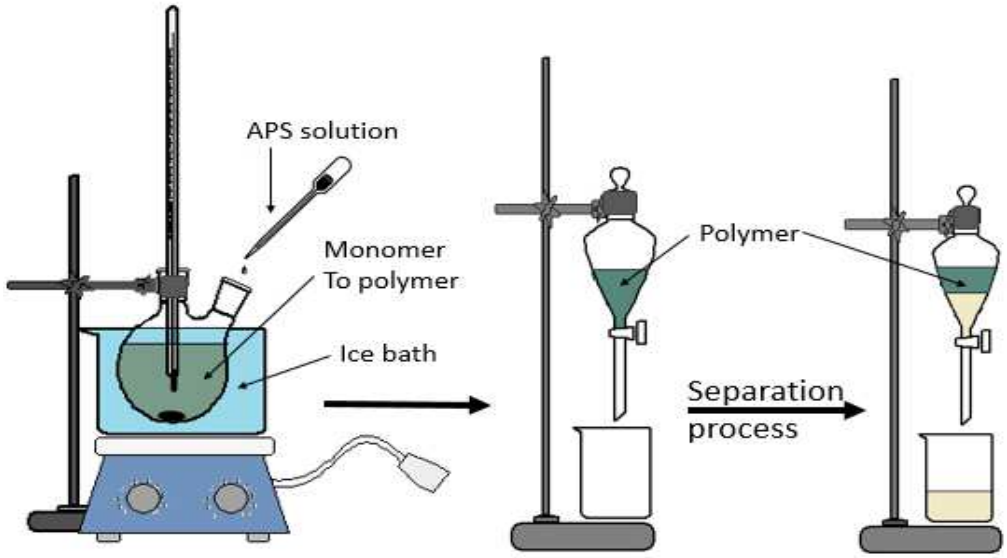

Figure 33: Schematic Diagram for PTPA and DBPA Synthesis Set Up.

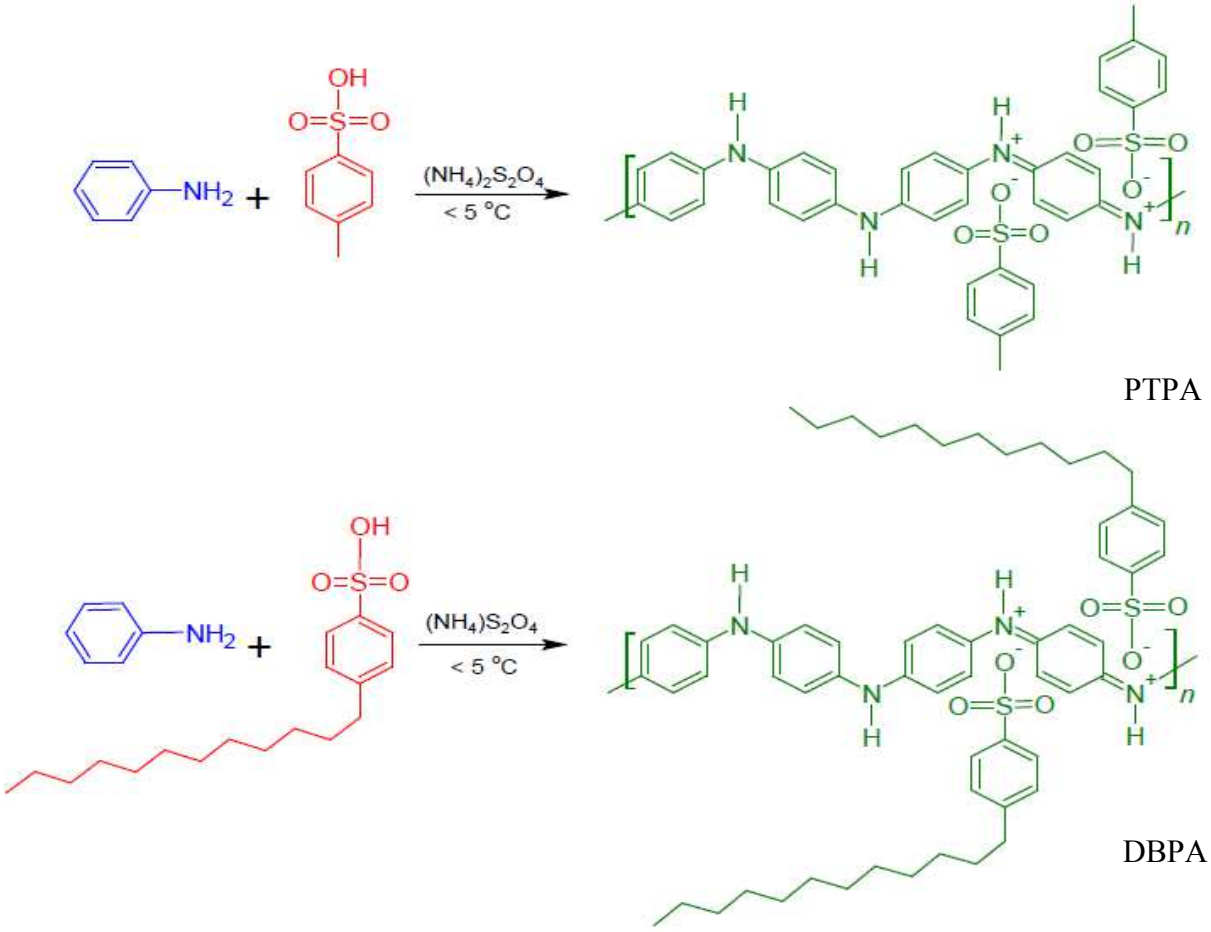

Figure 34: Chemical Reactions of Bulky Dopant Based Polyaniline.

3.3 Film Preparation:

Over the years, several coating techniques have been developed for preparing thin film including drop casting, spin coating and spray coating.[98, 99] **Figure 35** shows the most common coating techniques that were used in the laboratories for coating film.

Figure 35: Coating Techniques.

During the research, several coating techniques were tried to prepare the thin polymer films. Drop casting, dip coating and Dr. blade coating were the most successful methods. In drop casting, small amount of polymer solution was dropped on the glass substrate and then let the sample undisturbed.[98] The solvent was evaporated in the air leaving a thin solid film on the glass substrate as seen in **Figure 36**.

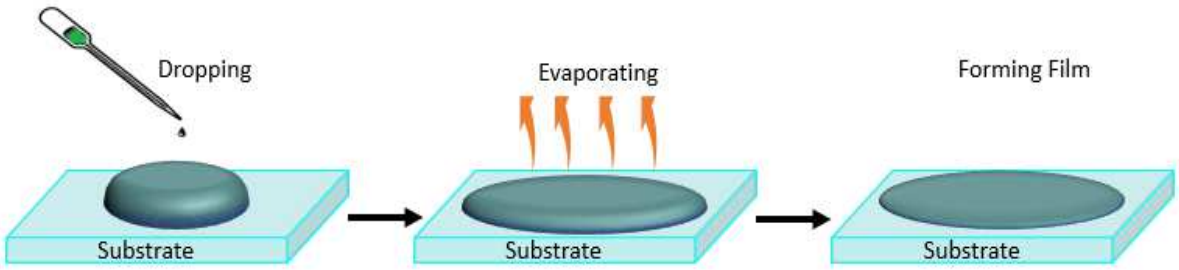

Figure 36: Schematic Diagram of Drop Casting Technique.

Dip coating was the second technique used in this experiment where liquid polymer sample was placed in a small glass container.[98, 99] Glass substrate was immersed in the polymer sample for a few second and then removed. The liquid sample was sticked on the substrate forming thin film **Figure 37** illustrates the dip coating process.

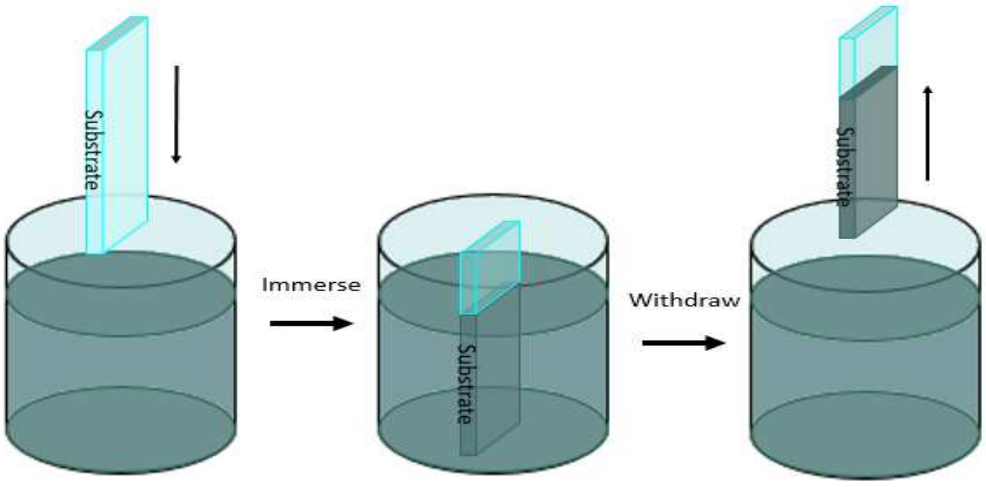

Figure 37: Schematic Diagram of Dip Coating Technique.

Dr. blade coating was also used during this research. In the Dr. blade coating processing 30 µl of the liquid polymer sample was dropped on a glass substrate.[98, 99] The droplet liquid was spread using a blade with 45-degree angle as seen in **Figure 38**. Then the sample left in the air to evaporate the solvent leaving a thin film behind on the glass substrate.

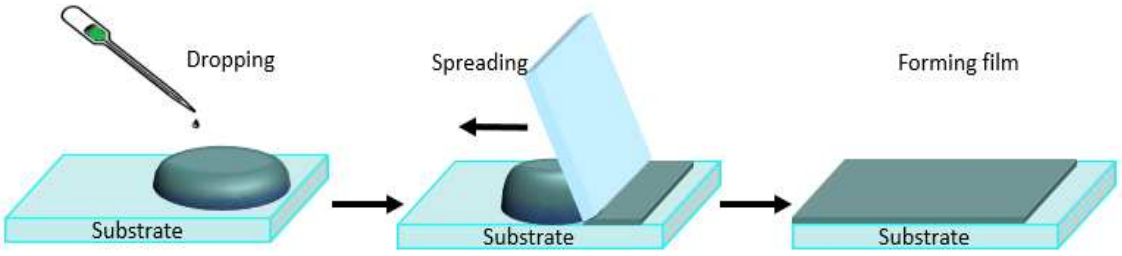

Figure 38: Schematic Diagram of Dr. Blade Coating Technique.

3.4 pH Solution Preparation:

Several pH solutions were prepared to investigate the pH effect on the solubility of polymers covering the pH from pH 1 to pH 13. Hydrochloric acid and sodium hydroxide are the two materials that have been used for the solutions preparation. PA.Cl, PA.F, PFA.Cl, PFA.PA.Cl and PSA.Cl were tested in the pH solution. That testing conditions were ultra-sonication for 5 min and 1 hour. The solutions were observed over night after the sonication.

3.5 Secondary Doping:

Several molecules were used for applying secondary doping process including *m*-cresol, thymol and *p*-TSA. **Figure 39** shows the chemical structures of the three dopants. Among the three dopants, *p*-TSA was expected to have higher impact including conductivity of the polymer due to the presence of the sulfonic group which has higher electron density than hydroxyl group. Thymol and *m*-cresol have similar chemical structures except for the branched alkyl group on ortho position in thymol which may cause a steric hindrance. The steric hindrance was expected to reduce the interaction between the hydroxyl group and the polymer.

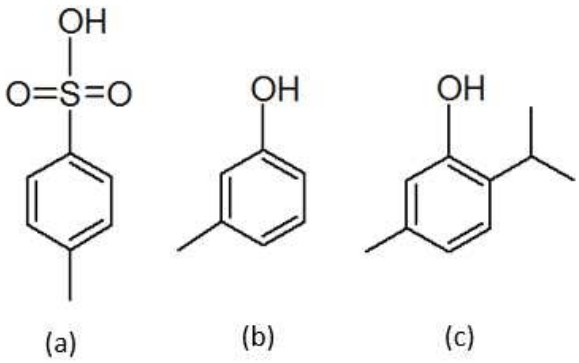

Figure 39: Chemical Structures (a) *p*-TSA, (b) *m*-Cresol and (c) Thymol.

3.5.1 Solution Doping:

Secondary doping solution was prepared using *m*-cresol in two concentrations of 2% and 5% *m*-cresol in DBPA. For *p*-TSA and thymol, the concentration was (W/V). Thin polymer films were prepared from the dopant/polymer solution using coating methods as describe previously.

Number of mole = volume x density/ m-cresol MW

Weight of the dopant (g) = Number of mole X the dopant MW

3.5.2 Film Doping:

For the secondary film dopants, *m*-cresol, thymol and *p*-TSA was used using concentration of 2% and 5% dopant in solvent. Previous procedure was used to prepare the dopant solution using several solvents including xylene, water, BuEt and blends of xylene and BuEt. Pre-fabricated DBPA polymer films were dipped in the dopant solution apply the secondary dopants to the film. **Figure 40** shows the solution and film doping for secondary dopant.

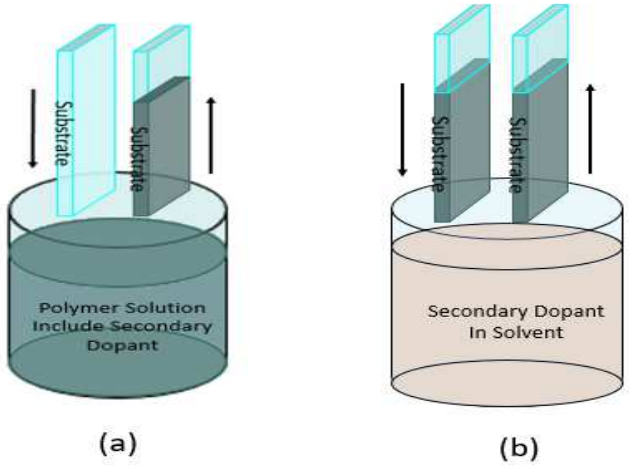

Figure 40: Schematic Diagram of (a) Solution Doping, (b) Film Doping.

3.6 Surface Resistance Measuring:

Surface resistance was measured using 2 probe method. Two bars of silver paint were applied on the film sample as shown in **Figure 41**. The multimeter probes were placed on the silver paint bars to read the surface resistance.

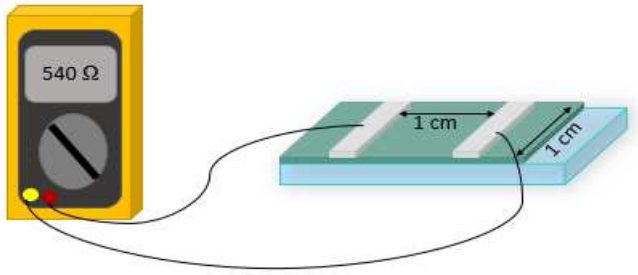

Figure 41: Scimatic Diagram of Surface Resistance Measurment.

3.7 Characterization Methods:

3.7.1 Fourier Transform Infrared Spectroscopy (FTIR):

The composition and structure of the polymers were characterized using the SHIMADZU-IR Prestige-21 model infrared spectrometer. The polymers structures were determined by grinding the sample with potassium bromide (KBr) and then pressed each sample into pellets at 3.5 psi of pressure for two minutes. Spectra were collected from wavenumber of 800-4000 $cm^{-1}$and the average scan number were 36.

3.7.2 Ultraviolet-Visible (UV-Vis) Spectroscopy:

The optical properties of each polymer were tested using SHIMADZU 2450 model UV-Vis spectrometer. The polymer samples were tested in solution and on solid film. In solution base, the polymers were dissolved in good solvent at different concentrations. For solid film,

polymer solution was casted in a glass plate using drop casting, Dr. blade coating or dip coating methods. The spectra were collected from the wavelength of 300-900 nm.

3.7.3 Proton Nuclear Magnetic Resonance (^{1}H NMR):

Proton nuclear magnetic resonance were also used for evaluating chemical structures of the synthesized polymers. SHUMADZU 4000 model (400 MHz) was used with a deuterated chloroform to collect the spectra using average scan of 68.

CHAPTER 4

RESULTS AND DISCUSSION

4.1 Primary Polymers Analysis:

4.1.1 The Effect of the Modification on the Solubility:

Modifying the polymer backbone with electron withdrawing atom including fluorine was observed to improve polyaniline solubility. On the contrast to polyaniline, poly(2-fluoroaniline) was found to be more soluble in so many organic solvents including THF, DMSO, DMF and NMP. **Figure 42** shows the pictures of polyaniline and poly(2-fluoaniline) in different organic solvents.

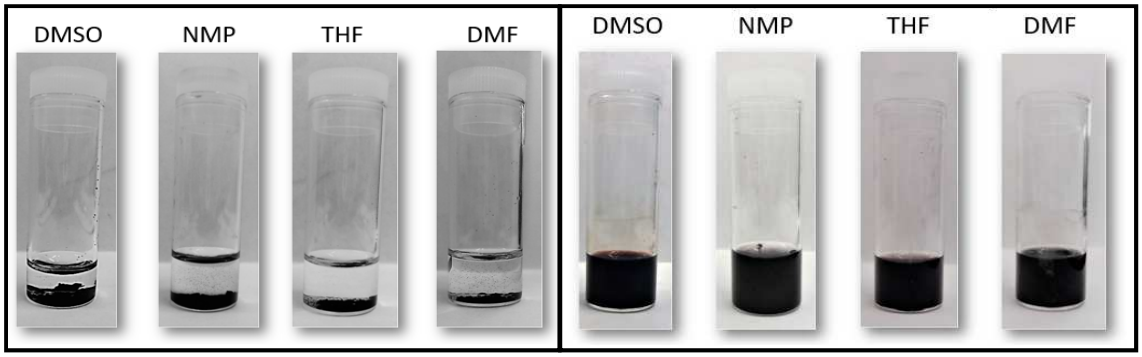

(a) (b)

Figure 42: (a) Polyaniline and (b) Poly(2-fluoroaniline) in Different Organic Solvents.

4.1.2 Effect of pH on Solubility and Optical Properties**:**

All primary polymers including PA.Cl, PA.F, PFA.Cl, PFA.PA.Cl and PSA.Cl were tested in aqueous solution of pH 1 to pH 13. The observation was conducted directly 5 min after added the polymers to the solution, after 5 min under ultrasonication, after 1 hour under ultrasonication and after left overnight undisturbed. The same pattern was observed for the other

polymer samples. Althought the polymers were observed to be dispersed in the solutions right after the ultrasonication, the polymers were precipitated overnight indicating the poor solubility of the polymer in water over the wide range of pH as seen in **Figures 43, 45, 47, 49** and **51**. UV-Vis absorption peak for all polymers at high pH value showed the blue shifted behavior which indicate that doped polymers were started to dedope and turn into bases losing the conductivity. **Figures 44, 46, 48, 50** and **52** illustrate the optical properties of the polymers in the solutions of different pH.

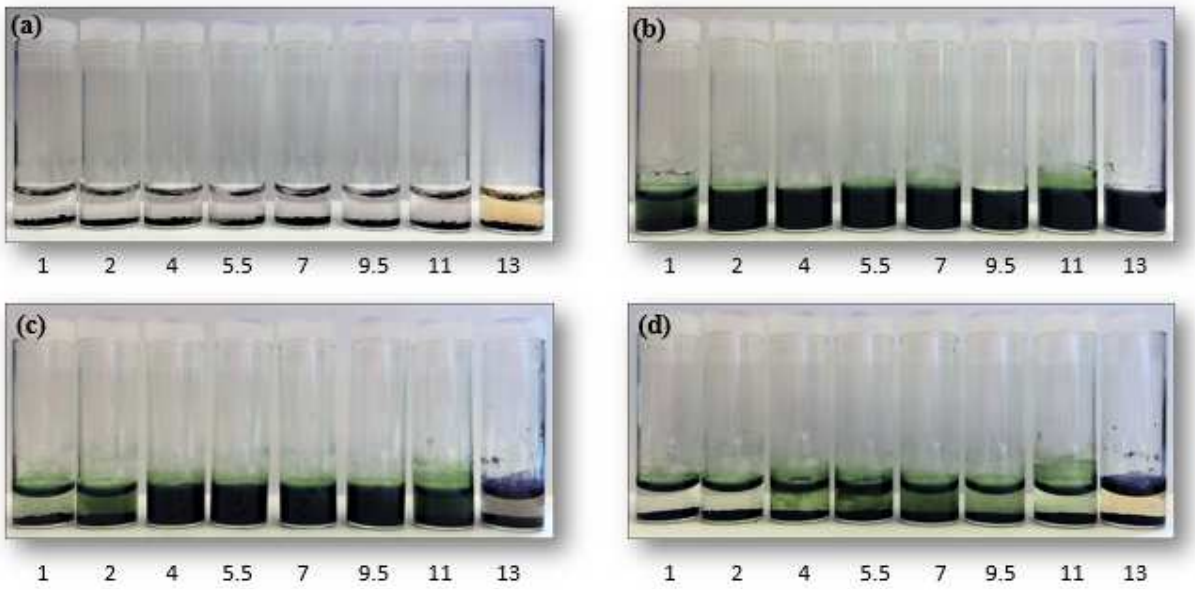

Figure 43: PA.CL in Different pH (a) Before Sonication, (b) After Sonication for 5 min, (c) After Sonication for 1 Hour and (d) After Overnight

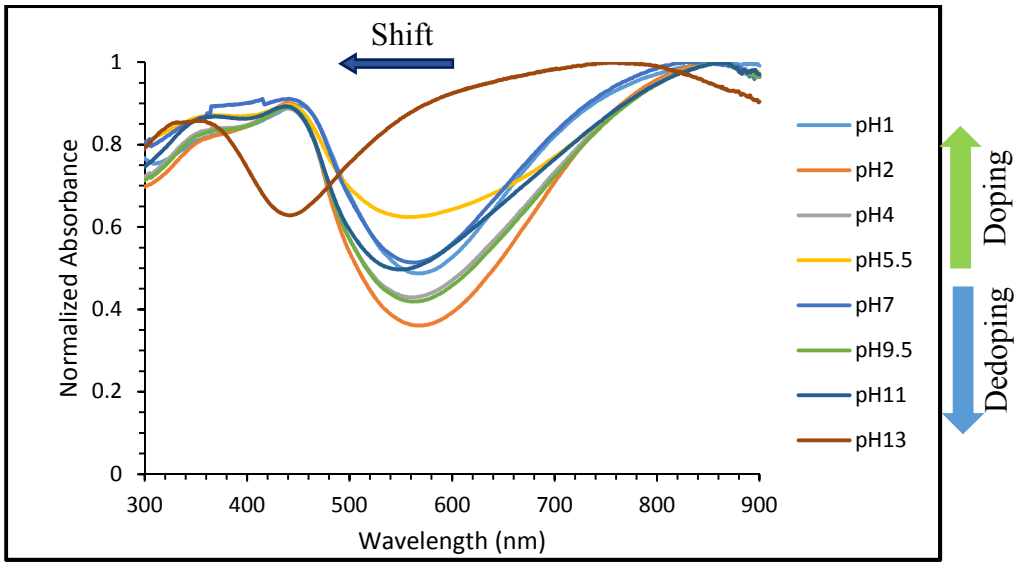

Figure 44: UV-Vis Spectra of PA.Cl in Different pH

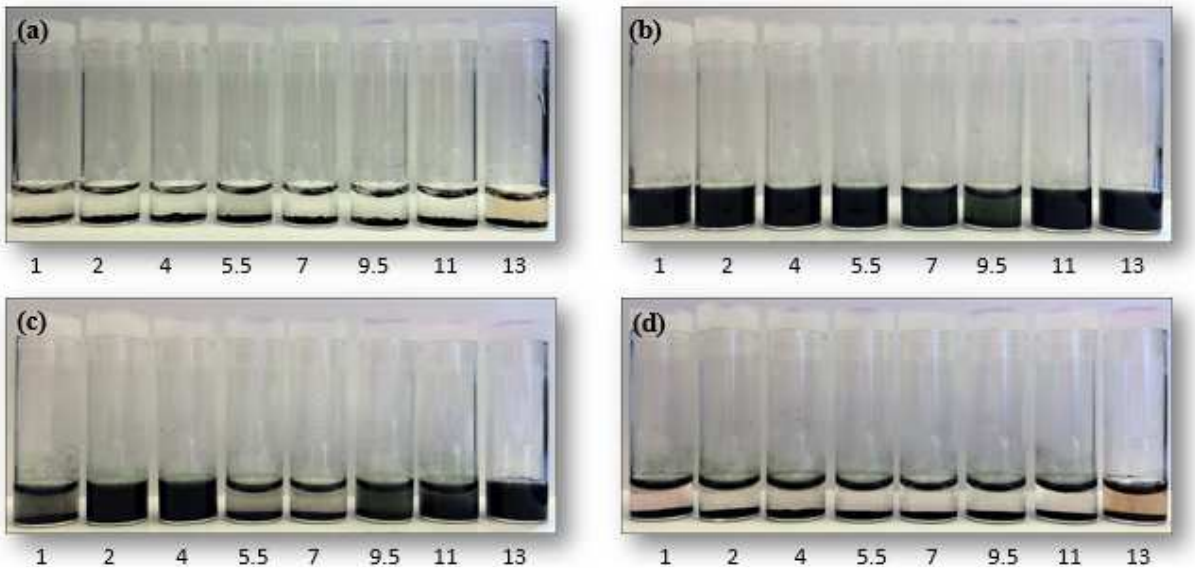

Figure 45: PA.F in Different pH (a) Before Sonication, (b) After Sonication for 5 min, (c) After Sonication for 1 Hour and (d) After Overnight

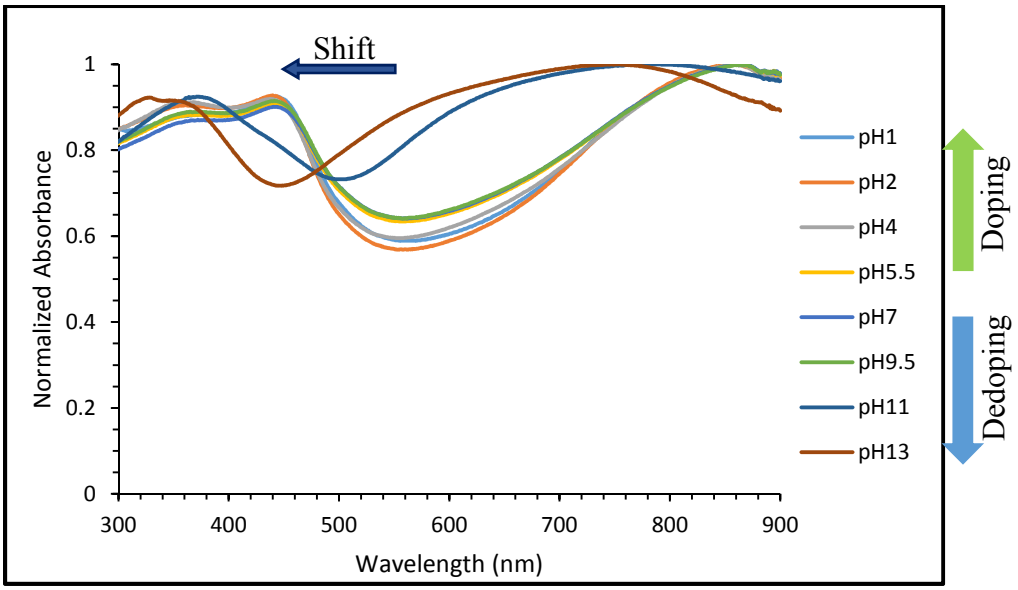

Figure 46: UV-Vis Spectra of PA.F in Different pH

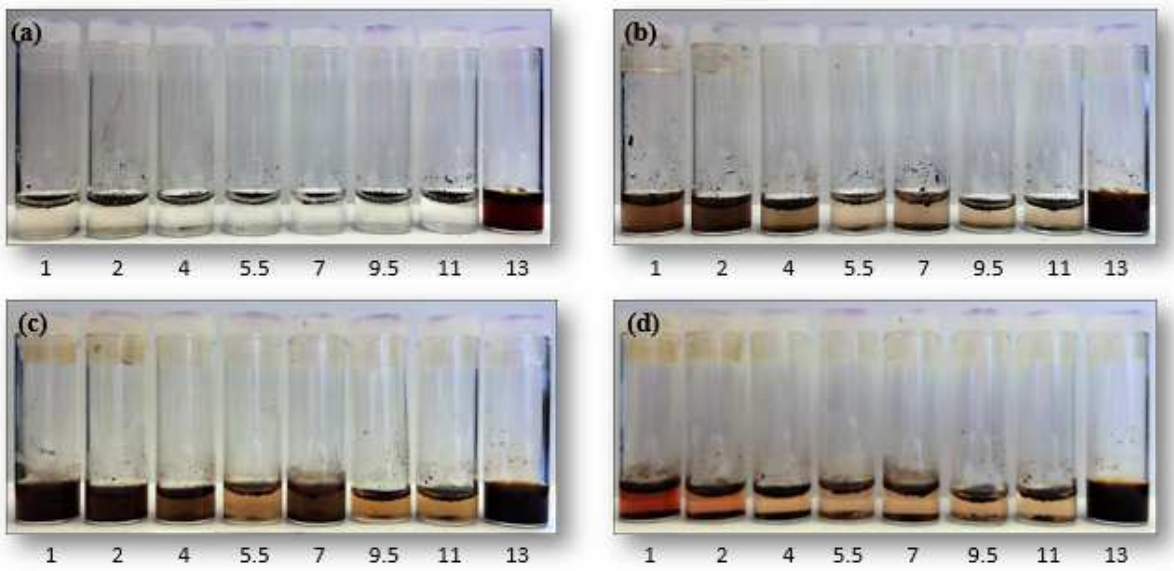

Figure 47: PFA.CL in Different pH (a) Before Sonication, (b) After Sonication for 5 min, (c) After Sonication for 1 Hour and (d) After Overnight

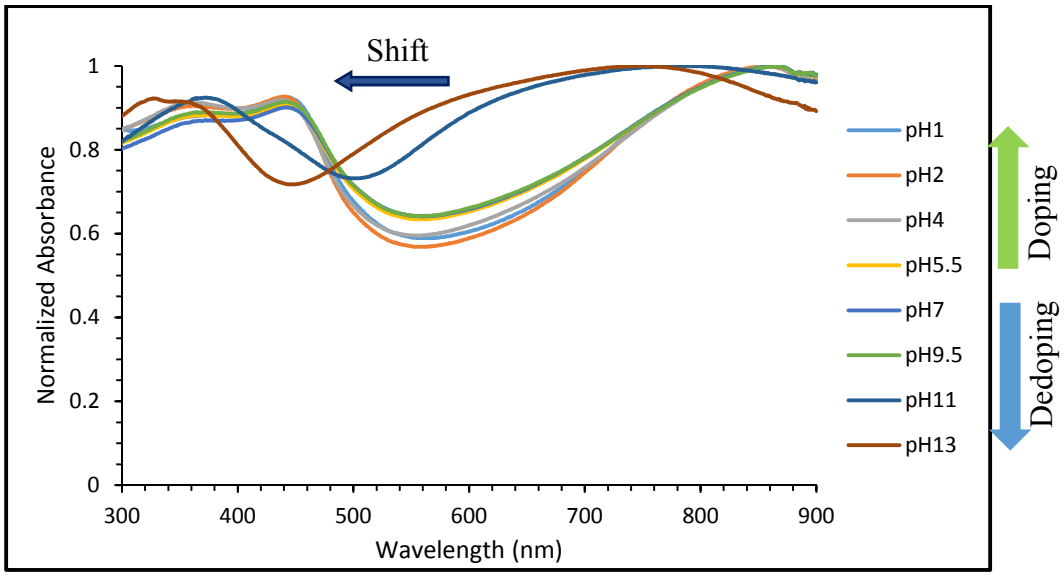

Figure 48: UV-Vis Spectra of PFA.Cl 42% in Different pH.

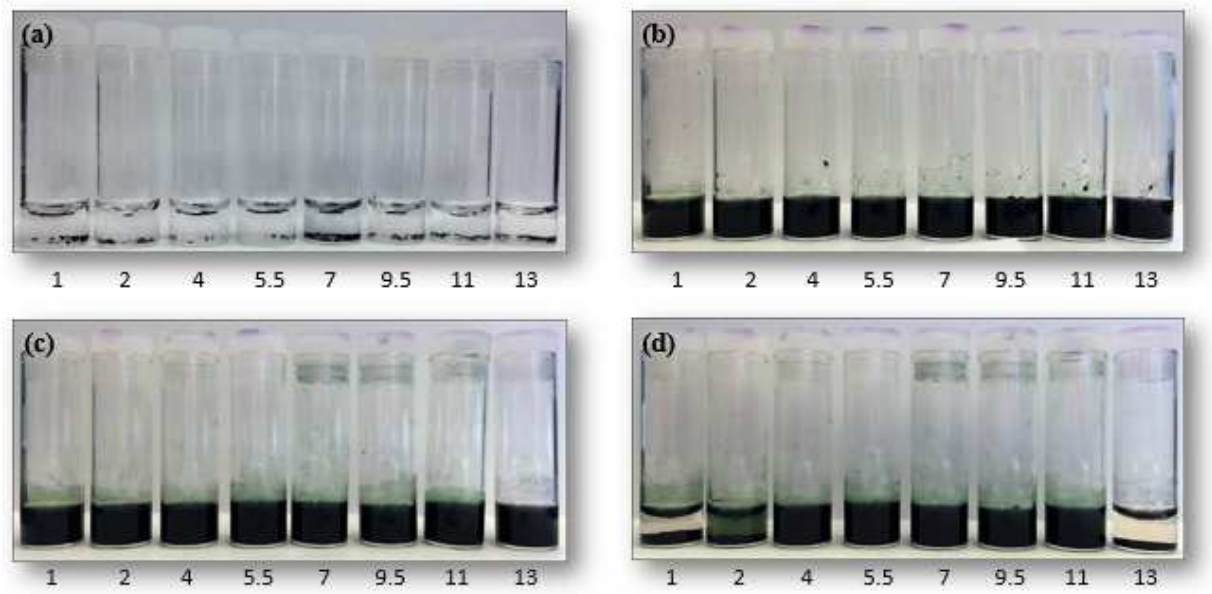

Figure 49: PFA.PA.CL in Different pH (a) Before Sonication, (b) After Sonication for 5 min, (c) After Sonication for 1 Hour and (d) After Overnight

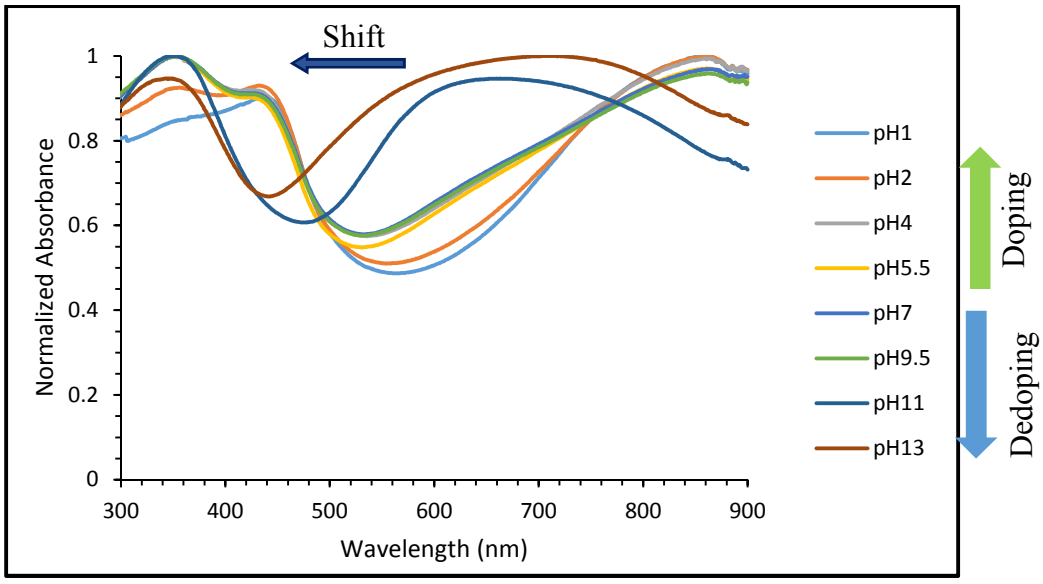

Figure 50: UV-Vis Spectra of PFA.PA.Cl in Different pH

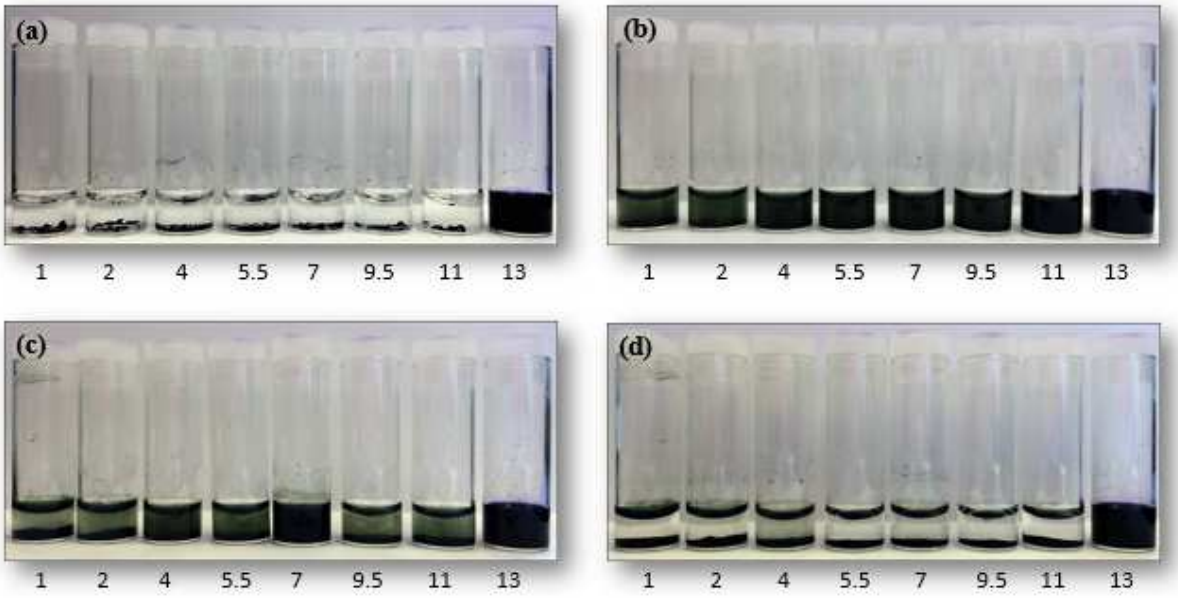

Figure 51: PSA.CL in Different pH (a) Before Sonication, (b) After Sonication for 5 min, (c) After Sonication for 1 Hour and (d) After Overnight

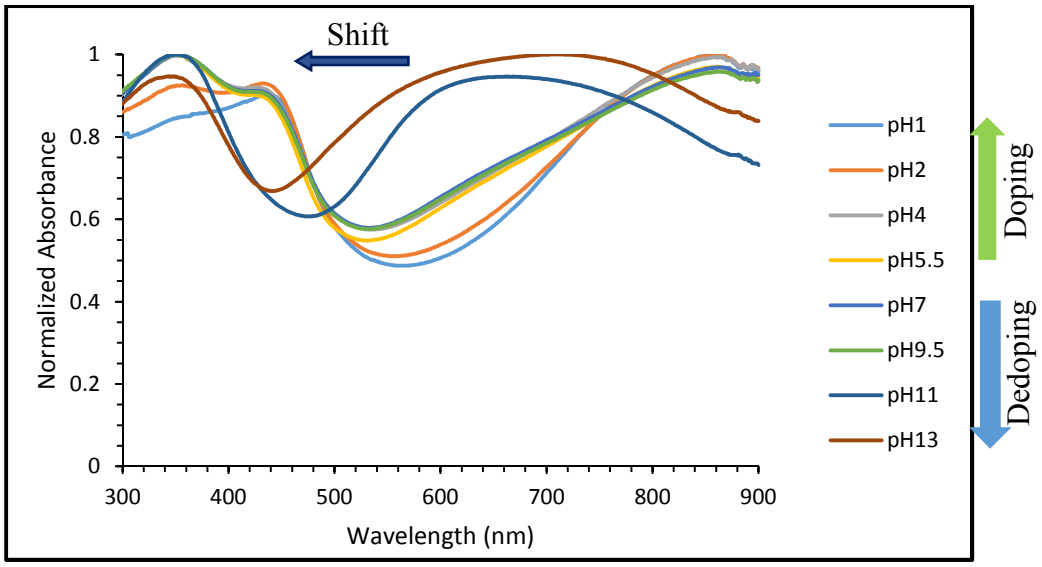

Figure 52: UV-Vis Spectra of PSA.Cl in Different pH

4.1.3 FTIR Spectra for Monomers and Polymers:

FTIR spectrometer was used to confirm the formation of polymers. As seen in **Figure 53** the peaks at 1580 and 1500 cm^{-1} are the characteristic peaks of polyaniline, which are assigned to the C=C ring stretching of the quinoid and benzoid unites in the backbone structures, respectively. The peaks at 1290 and 1120 cm^{-1} are corresponding to vibration of C−N and N− Cl at almost all polymers confirming the formation of doped polymers. For poly(2-fluoroaniline), there is a characteristic peak at 1215 cm^{-1}confirming the presence of C− F bond. The peaks at 1207 and 1058 in sulfonated polyaniline are assigned as asymmetric, symmetric stretching modes of O−S−O, respectively. The peak at 697cm^{-1} is corresponding to C−S which confirmed the formation of sulfonic group on the polymer benzene ring.

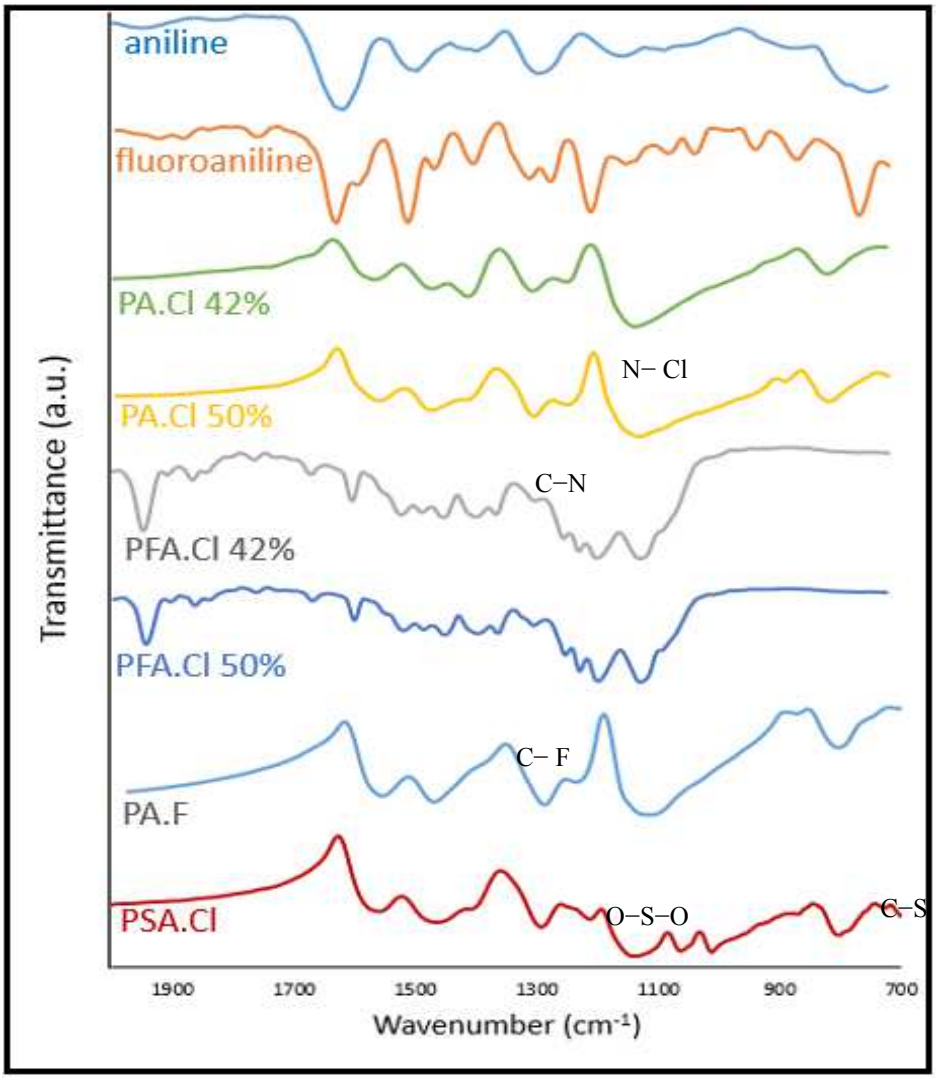

Figure 53. FTIR for The Polymers and The Monomers.

4.1.4 UV-Vis Spectra of Poly(2-fluoroaniline):

UV-Vis spectra were collected for partially and fully doped poly(2-fluoroaniline) in thin film before and after thermal treatment. The films were fabricated using Dr. blade coating method from the polymer and THF solution. The thermal treatment has been done using 150 ^{O}C for 30 min. As seen in **Figure 54** and **Figure 55** which represents the partial and full doping of

PFA.Cl respectively, the absorption intensity was reduced after the thermal treatment. The reduction of the peak intensity is an indication of increasing the crystallinity or the degree of extension of entangled molecules in the polymer film which can be beneficial for improve the conductivity of the polymer.

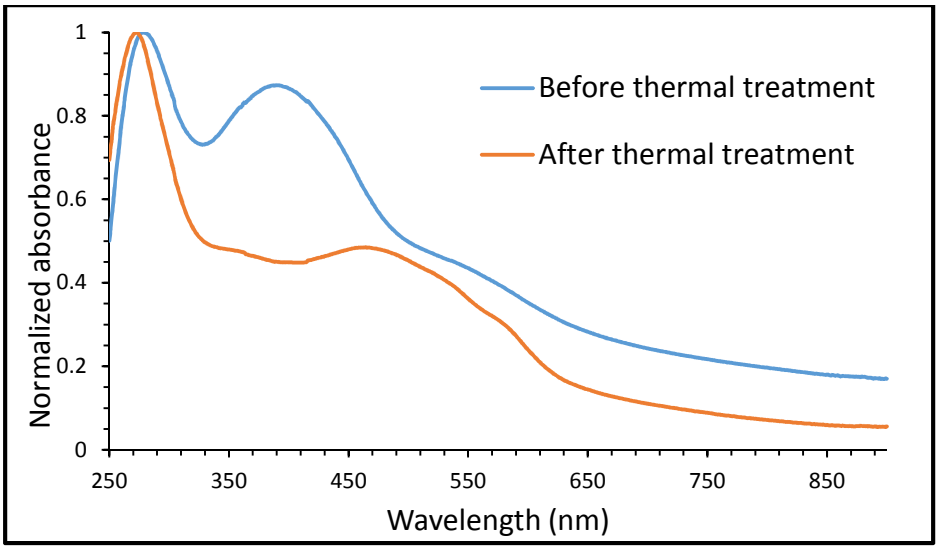

Figure 54: UV-Vis Spectra of PFA.Cl 42% in Film Before and After Thermal Treatment.

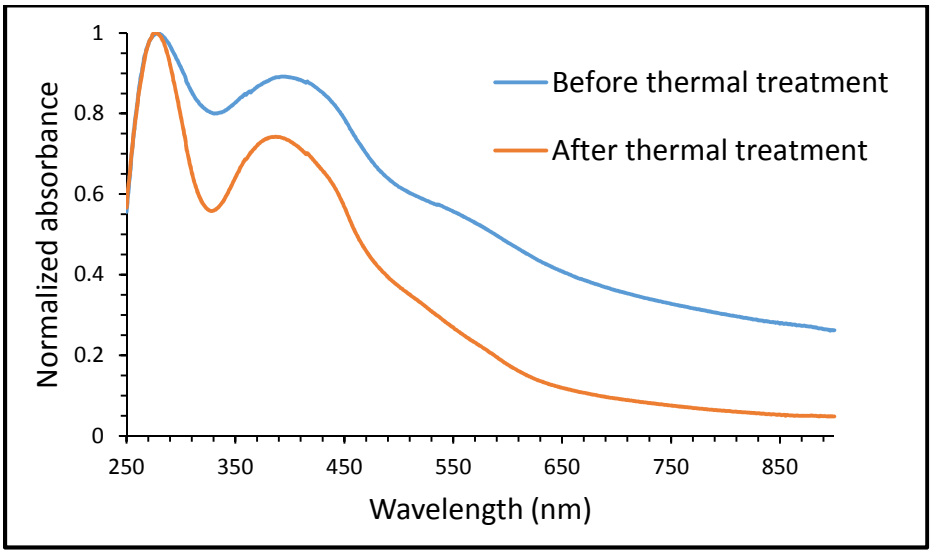

Figure 55: UV-Vis Spectra of PFA.Cl 50% in Film Before and After Thermal Treatment.

4.2 DBPA and PTPA Analysis:

4.2.1 ^{1}H NMR Spectra:

^{1}HNMR was performed for DBPA, DBSA monomer and aniline using chloroform D as a solvent. The obtained spectra confirmed the polymerization of polyaniline doped with DBSA. **Figure 56** shows three different types of peaks appeared between 6.5 - 7.5 ppm which are assigned for the different protons on the benzene group of aniline. These three types of proton are reduced to one type in the DBPA which confirmed the formation of the polymer since benzene ring in the polymer has equivalent protons as seen in **Figure 57**. In addition, the peak around 3.4 ppm which represents the proton on – NH_2 group. The intensity of – NH_2 peak is reduced in the spectra of the polymer and limited to the end group only.

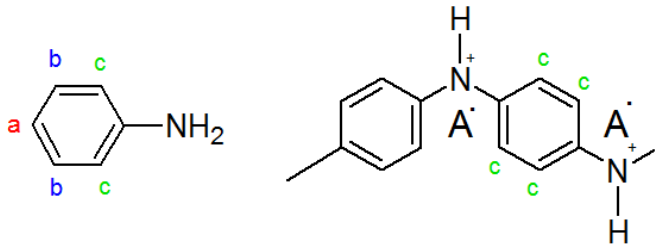

(a) (b)

Figure 56: Types of Proton in Benzene Ring (a) Aniline and (b) Polyaniline.

For DBSA, there are multiple characteristic peaks around 0.8 ppm which are assigned to the long chain of the alkyl group (methylene R− CH_2−). Another peak at 1.7 ppm which is assigned to the methyl group at the end of the alkyl chain (R−CH_3). Please note that those peaks are moved to the DBPA polymer spectra which identifies the doping confirmation of the polymer with DBSA. The peak appearing at 11.4 ppm in the DBSA spectra represents S−O−H group. It is

noticeable that this peak is disappeared in the DBPA spectra due to the elimination of the O−H group during the doping process. On the other hand, another peak started to appear around 3.7 ppm on DBPA spectra due to the formation of – NH^+ confirming the polymerization.

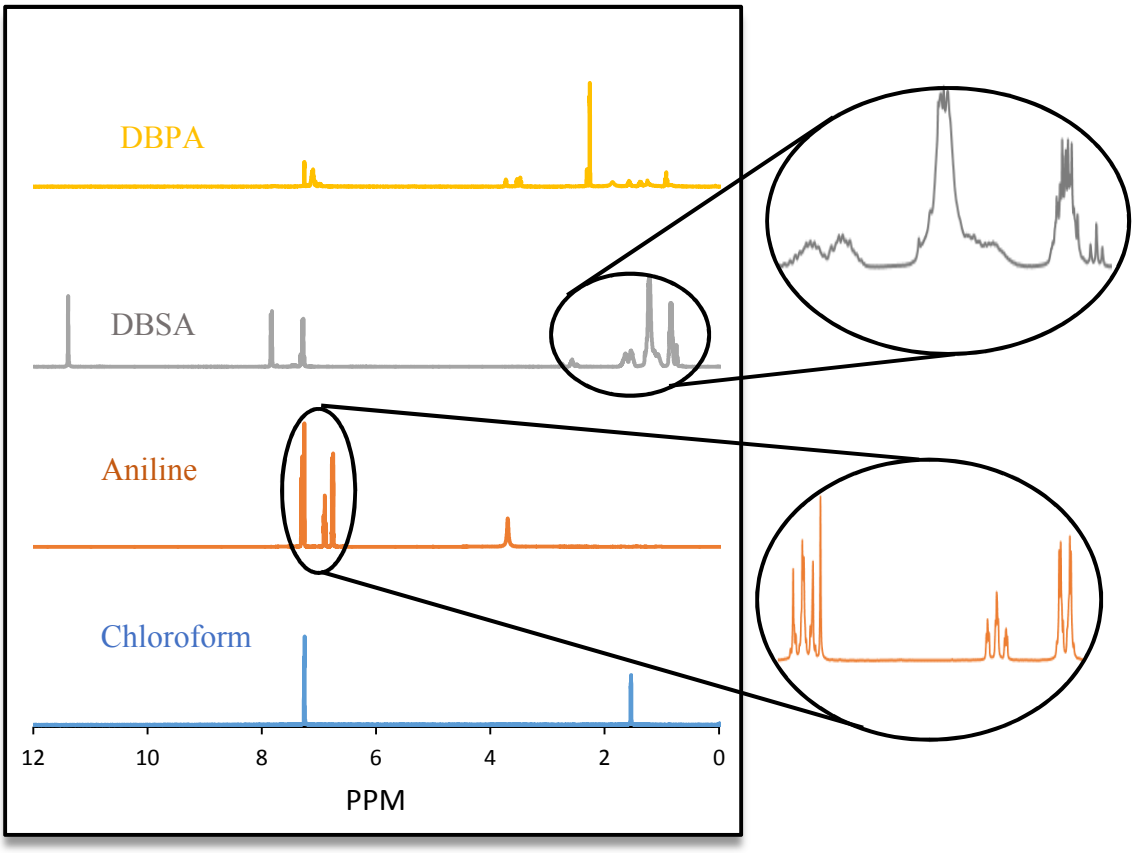

Figure 57: ^{1}HNMR Spectra for Chloroform, Aniline, DBSA and DBPA.

4.2.2 FTIR Analysis:

Analyzing the FTIR spectra for both DBPA and PTPA confirms the doping of polyaniline with DBSA and *p*-TSA. Similar peaks appeared in both polymers due to the similar chemical structure in the dopants *p*-TSA and DBSA as seen in **Figure 58**. The peaks including 1030, 1122, 1220 and 1400 cm^{-1} which are referred to asymmetric and symmetric stretching modes of O−S−O, CH_3 and N−O, respectively. Also, the characteristic peaks for benzoid and

quinoid units in the polymer backbone at 1470 and 1575 cm^{-1} are appeared in both polymers. There is a peak that appears only in DBPA spectra at 1300 cm^{-1} which is assigned for the long alkyl chain on the tail of DBSA. **Figure 58** shows the characteristics peaks for the two PTPA and DBSA polymers.

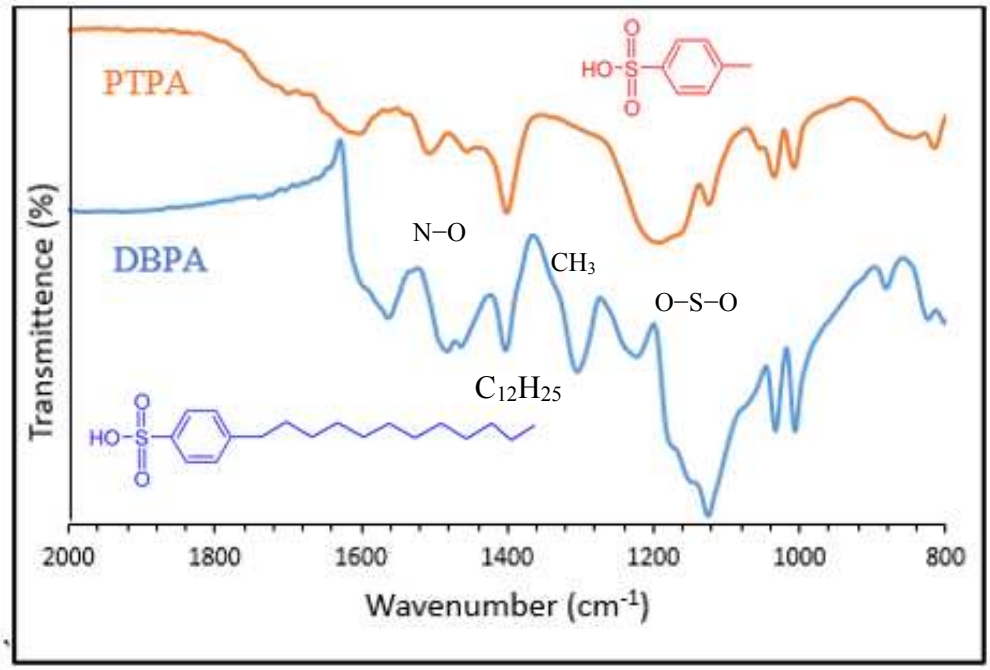

Figure 58: FTIR Spectra of DBPA& PTPA

4.2.3 UV-Vis Analysis:

Figure 59 shows UV-Vis spectra of DBPA in solution and film before and after thermal treatment. The films were fabricated using drop casting and dip coating techniques. Thermal treatment was applied at 150^{O} C for 30 min. There is reduction in the intensity of absorption peak between 675-875 nm was observed on film spectra after the thermal treatment compared to before thermal treatment. That reduction was occurred due to the same reason which is improved

the delocalization of charge via molecular alignment of the polymer chains after the thermal treatment.

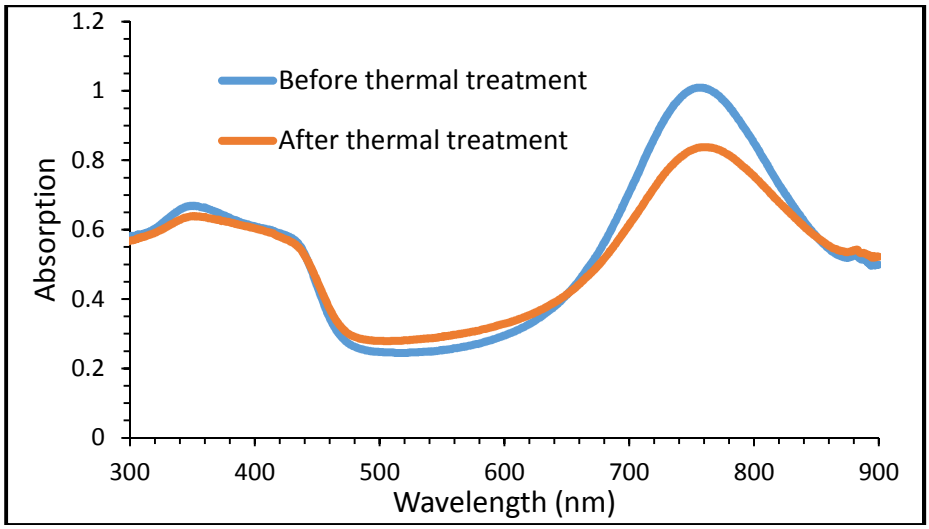

Figure 59: UV-Vis Spectra of DBPA in Film Before and After Thermal Treatment.

UV-Vis spectra of the DBPA solution in xylene and film are collected where **Figure 60** (**a**) present the processed data and the normalized data are presented at **Figure 60** (**b**) to illustrate the reduction percentage. The absorption peak intensity of the DBPA spectra between 675-875 nm was observed to be reduced from solution to film. This reduction as mentioned earlier is due to improve the alignment of the polymer backbones and increase of the crystallinity in the film polymer more than solution.

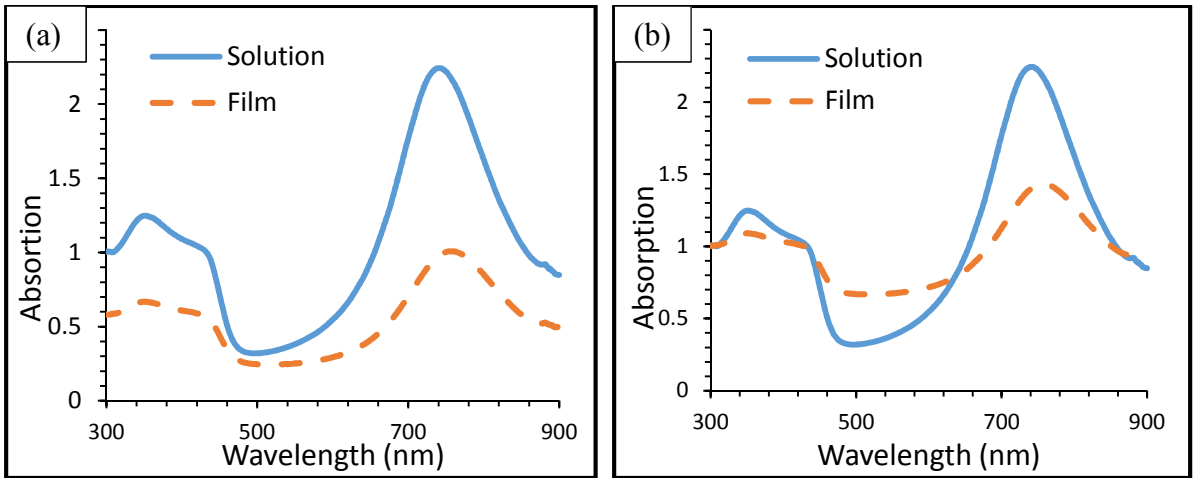

Figure 60: UV-Vis Spectra of DBPA in Xylene Solution and Film.

4.2.4 The Polymer Solubility:

It was observed that the solubility was improved significantly with changing the counter anion size. DBSA has similar chemical structure compared to *p*-TSA having long alkyl chain (dodecyl group) while *p*-TSA has the methyl group as seen in the **Figure 61**. Which prove to improve the solubility.

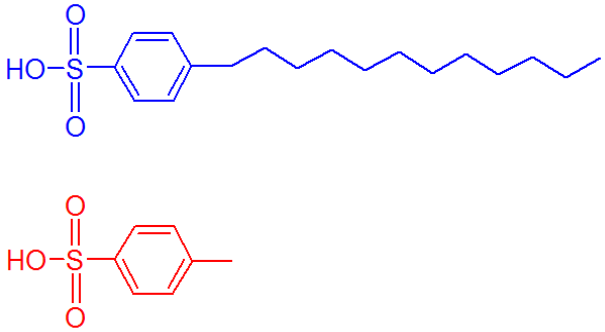

Figure 61: Chemical Structure for DBSA and *p*-TSA.

The intermolecular space between the polymer chains variation is one of the main factors that control the polymer solubility. Increasing that space may leads to loosen the polymer chains staking so the solvent molecules can penetrate between the chains to interact with the individual

molecule. Introducing a larger or bulky size dopant can be beneficial to increase the intermolecular space according to dopant size resulting to improve the solubility and electronic conductivity correspondingly. That was observed in DBPA when DBSA with long alkyl group replaced the *p*-TSA with short methyl group in PTPA. DBPA was found to have good solubility in several organic solvents including xylene, chloroform and toluene while PTPA showed poor solubility in most of the solvents. **Figure 62** shows the effect of the *p*-TSA and DBSA sizes on the intermolecular space between the chains of the polymers.

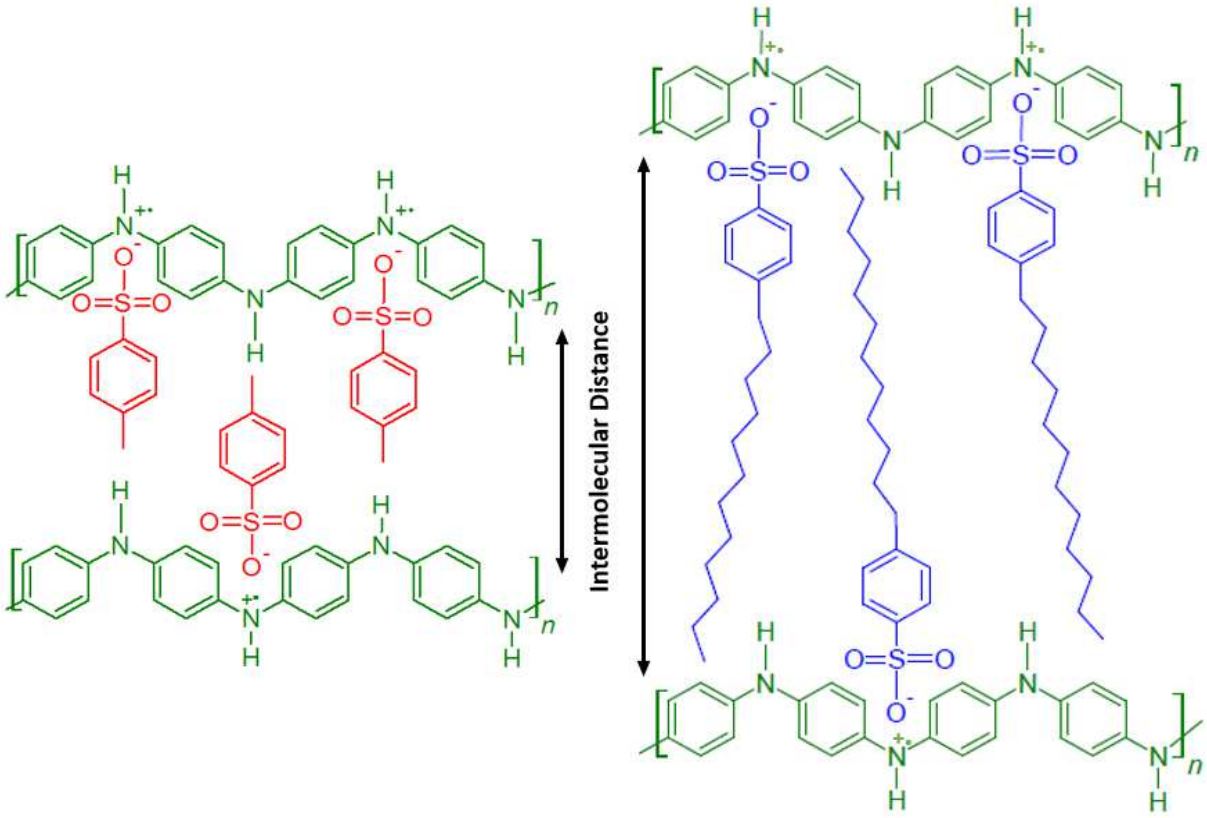

Figure 62: Intermolecular Space of PTPA and DBPA.

4.2.5 Secondary Doping:

During this research three different dopants were chosen to be used as secondary dopant which were *p*-TSA, *m*-cresol and thymol. The secondary dopants were applied into solution and film doping. **Figure 63** depicts the chemical structures of the three dopants and its attached groups.

As expected, *p*-TSA showed significant impact on improving the electrical properties because of the high electron density on the reducing sulfonic group over hydroxyl group of *m*-cresol and thymol. The high electron density increases the electrostatic attraction between the counter anion and the cationic site on the polymer backbone. Although *m*-cresol and thymol have the same reducing hydroxyl group and similar chemical structure, *m*-cresol has better impact on the surface resistance over thymol. Extra branched alkyl group (isopropyl group) that located at ortho position on thymol may causes steric hindrance between the dopant and the polymer backbone which cause distortion to the polymer chains and lower the ability of thymol to bind to the polymer backbone. Accordingly, the electron flow along the polymer backbone blocked which cause increasing in the surface resistance and reducing the electrical conductivity of the polymer.

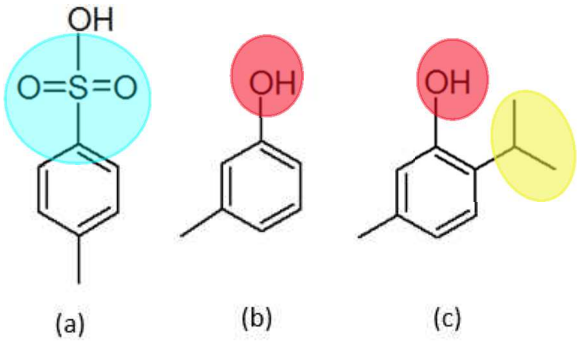

Figure 63: Chemical Structures and the Attached Functional Groups (a) *p*-TSA, (b) *m*-Cresol and (c) Thymol

4.2.6 Surface Resistance:

The surface resistance for the original DBPA, before water trace removal, was tested to be 6 MΩ/□. Several techniques were applied to get rid of the unwanted water that was trapped in the polymer solution including rotatory evaporator and applying drying agent. Then the surface resistance was tested after thermal treatment for 30 min at 150 ^{O}C. Significant improvement was observed regarding the surface resistance which was found to be 16 KΩ/□. The surface resistances were recorded after applying both solution and film doping to the DBPA polymer with post-treatment using the multimeter as discussed earlier.

4.2.6.1 Surface Resistance for Solution Doping:

The solution doping was prepared using 2% and 5% of the secondary dopant including *p*-TSA, *m*-cresol and thymol. The teste was performed on the film after thermal treatment under 150 ^{O}C for 30 min. The surface resistance showed significant reduction with *p*-TSA due to the structure variation as discussed earlier. **Figure 64** showed the values of the surface resistance for the three secondary dopants after post treatment compared to the DBPA without the secondary doping. By using the solution doping, the surface resistance has found to be decreased from 16 KΩ/□ to 0.7 KΩ/□ using 5% *p*-TSA.

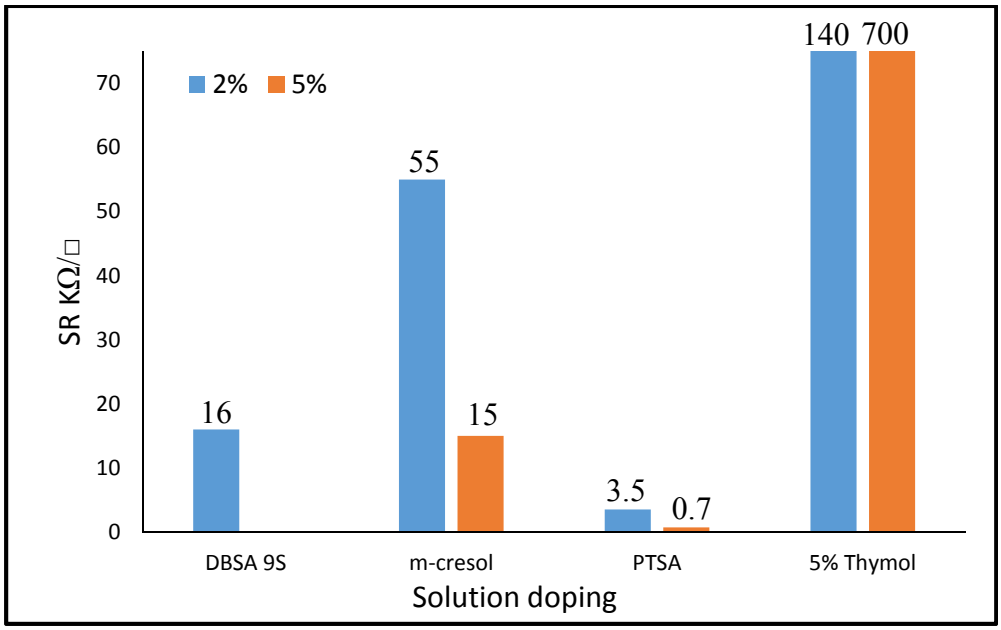

Figure 64: Surface Resistance for Solution Doping.

4.2.6.2 Surface Resistance for Film Doping:

The surface resistance for DBSA in film doping was also performed using the three secondary dopants investigating different parameters that was expected to affect the surface resistance. The dopant concentration in the solution is one of the major parameters that was investigated. **Figure 65** shows the surface resistance using *m*-cresol with 5 and 10% (V/V) in xylene after thermal treatment for 30 and 60 min at 150 ^{O}C. It was clear that the *m*-cresol with 5% has better impact compared to 10%. It is also noticeable the thermal treatment duration is another factor that affecting the resistance. Heat treating for 30 min showed better result with big reduction from 16 KΩ/□ to 8.5 KΩ/□.

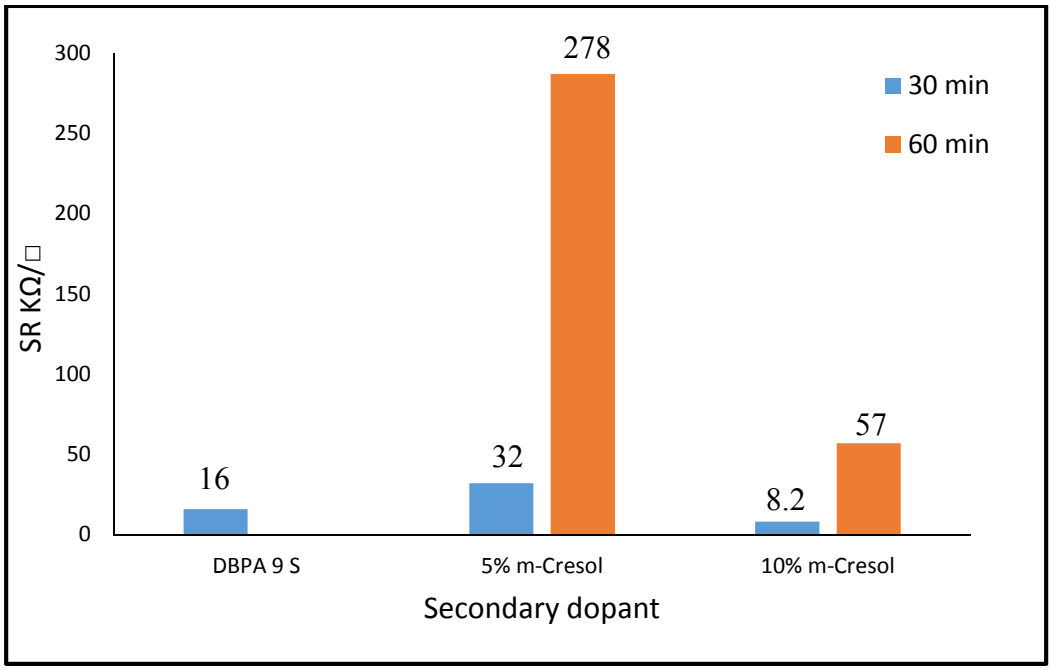

Figure 65: Surface Resistance for Film Doping.

Although, thymol was found to increase the resistance in solution doping but it was performed in film doping to emphasize the doping concentration effect. 2%, 5% and 10% thymol (W/V) in xylene was used with 30 and 60 min thermal treatment. **Figure 66** shows the collected data and unexpectedly it shows reduction in the surface resistance for 5% thymol with 30 min thermal treatment from 16 KΩ/□ to 10.6 KΩ/□.

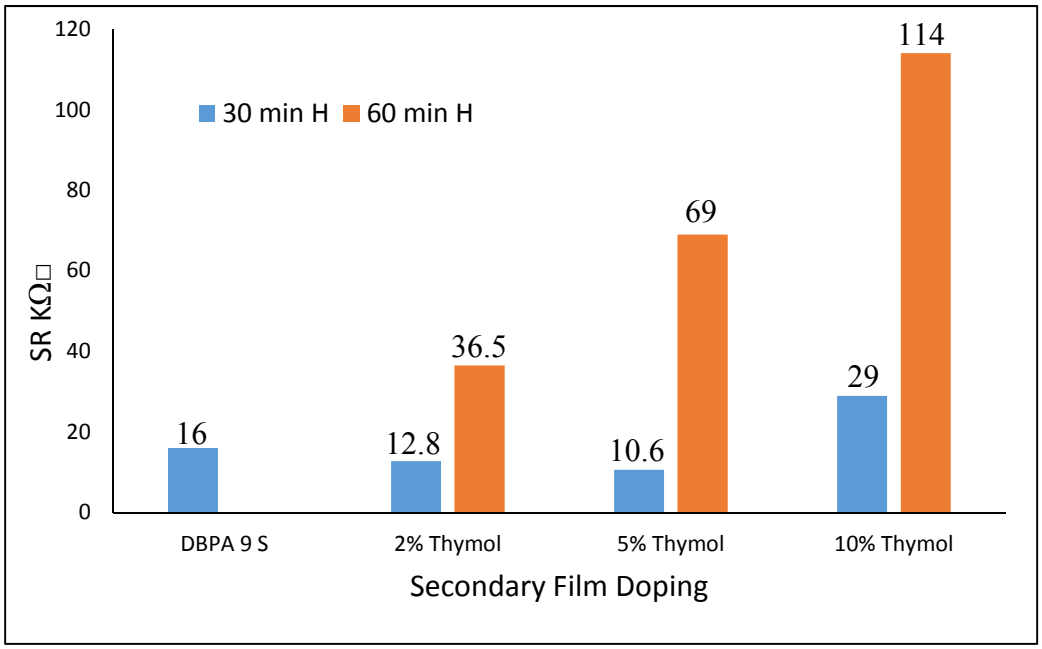

Figure 66: Surface Resistance for Film Doping with Thymol.

Using *p*-TSA as a secondary film dopant was expected to show big reduction in surface resistance as in solution doping. another factor was investigated which is the solvent effect as well as the concentration and the thermal treatment. Two set of solutions was prepared with 2% and 5% *p*-TSA in different solvents including water, xylene, BuEt, 5:1 xylene: BuEt and 5:2 xylene: BuEt. **Figure 67** shows the surface resistance for 2% *p*-TSA film doping in the five solvents using 30 min and 60 min thermal treatment at 150 ^{O}C. In the film doping, *p*-TSA proved to have the best impact on the surface resistance. By using 2% *p*-TSA dissolved in 5:1 xylene: BuEt, the surface resistance was reduced significantly from 16 KΩ/□ to 0.65 KΩ/□.

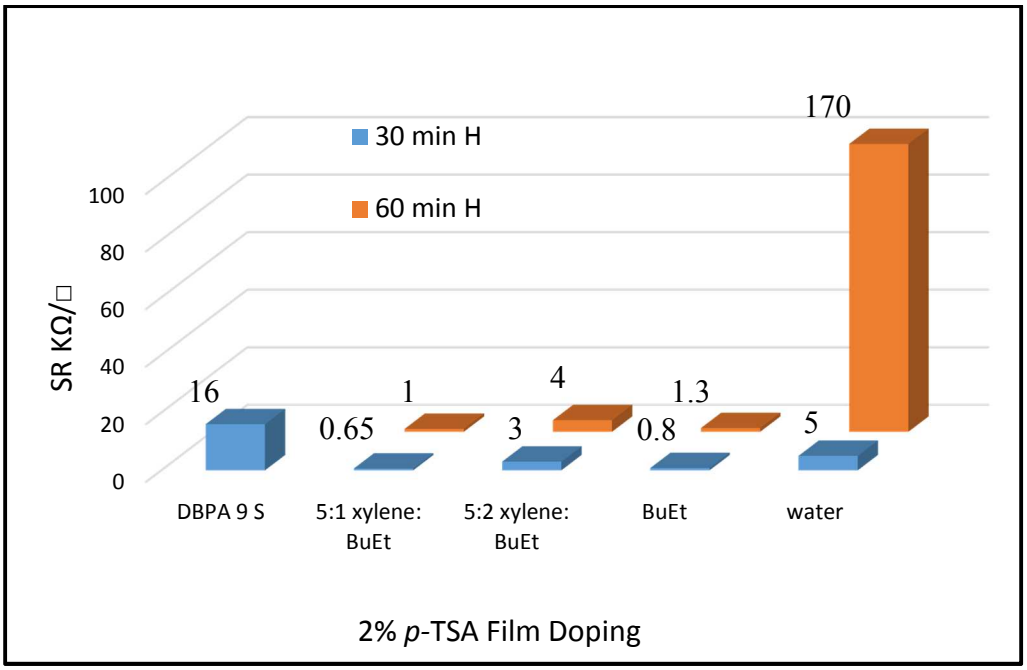

Figure 67: The Surface Resistance for Film Doping with 2% *p*-TSA

Almost the same pattern was observed when 5% *p*-TSA used in film doping in the different solvents. Although all solvents showed a big improvement regarding the surface resistance, using xylene: BuEt as co-solvent prove to be the most promising solvent for *p*-TSA as film dopant. **Figure 68** shows the surface resistance for DBPA film doped with 5% *p*-TSA in different solvents compared to the DBPA without the film doping.

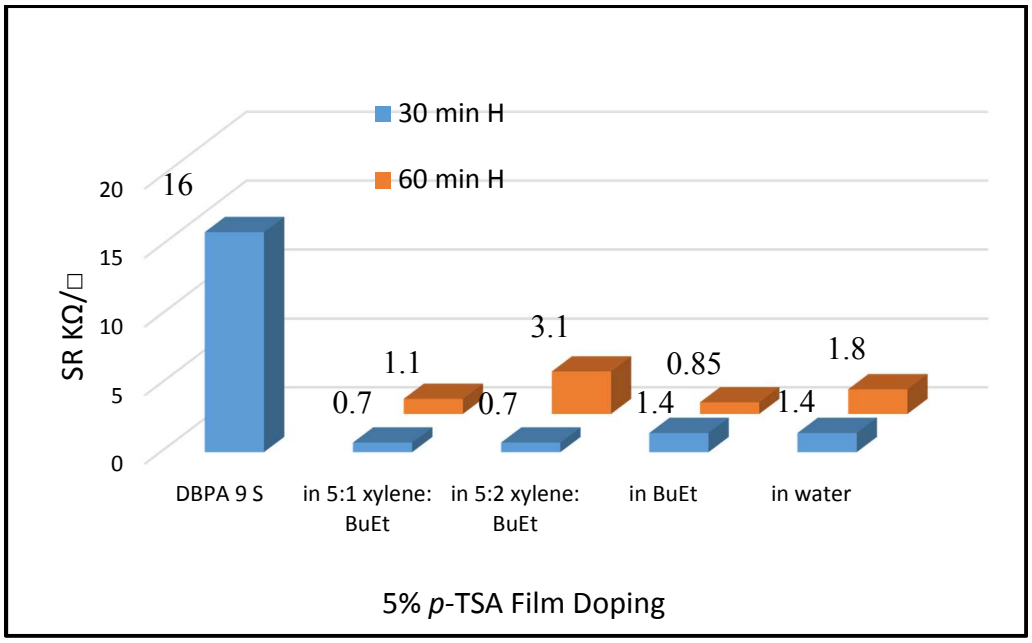

Figure 68: The Surface Resistance for Film Doping with 5% *p*-TSA.

All the previous data for solution doping and film doping under thermal treatment for 30 and 60 min for the 5% concentration of the three dopants have been collected in **Figure 69**. The comparison illustrates that in all cases *p*-TSA to have the best impact on the surface resistance as a secondary dopant.

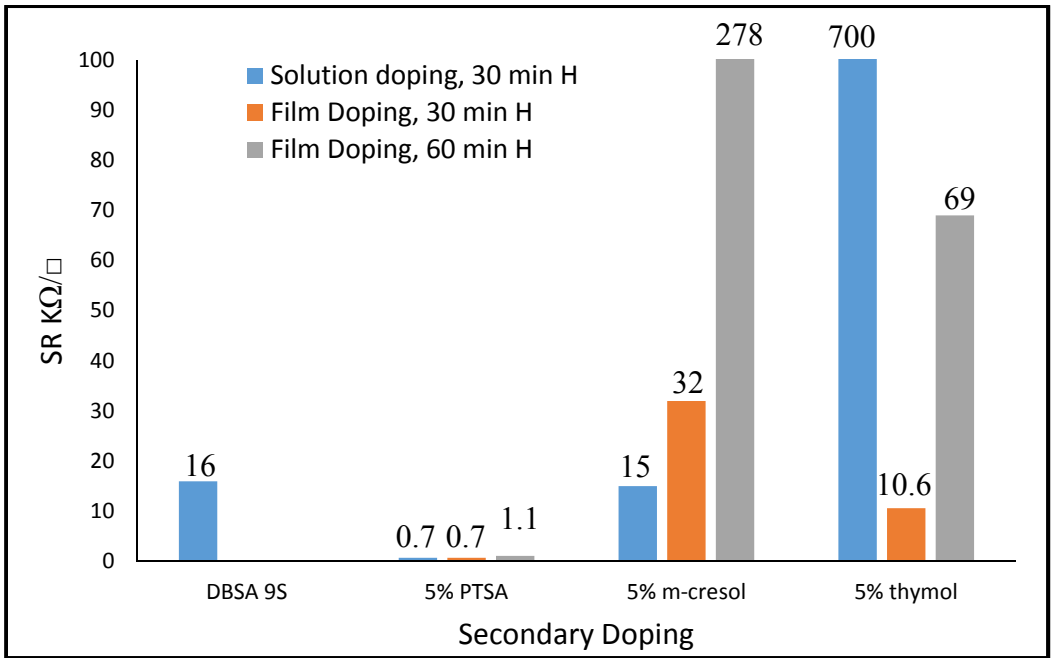

Figure 69: The Surface Resistance Solution and Film Doping.

CHAPTER 5

CONCLUSION

5.1 Discussion:

The objective of this work is to synthesize and to characterize ICPs having improved electrical properties as well as solubility. Series of polyaniline as one of the most promising polymers was successfully synthesized using oxidative polymerization along with APS as oxidant. In general polyaniline exhibits a poor solubility in organic solvents. So, studying the intermolecular interaction was necessary to improve the solubility of the polymer. One of the approach that proved to have good impact on the solubility was to introduce an electron withdrawing atom in the polymer backbone including fluorine atom and/or sulfonic group. Poly(2-fluoroaniline) was synthesized using 2-fluoroaniline monomer along with HCl as a counter anion. Due to the introduction of the fluorine atom, corresponding solubility of the polymer was measured to show huge improvement in organic solvents including DMSO, THF, NMP and DMF.

The other objective is to investigate the inter-relationship between the structure and electrical properties of ICPs. Polyaniline was previously reported and studied well using small-sized counter anion including HCl and HF. In order to improve the solubility without affecting the electrical conductivity, another approach was to use bulky counter anions. The dopants were expected to loosen the tight stacking of the polymer chains, for which two similar chemical-structured counter anions were chosen, *p*-TSA and DBSA. The polyaniline that was synthesized using DBSA as counter anion showed significant improvement in the solubility in organic solvents including xylene, toluene and chloroform. While the polymer was synthesized using

p-TSA, the limitation in the solubility was observed due to the existence of small-sized spacer that is short methyl group. The impact of the small spacer was assessed comparing to analogous dodecyl group of the DBSA.

In order to test the surface resistance for the polymer, several coating techniques were used to fabricate the polymer thin film including drop casting, dip coating and Dr. blade coating. The original polyaniline doped with DBSA was very difficult to collect the polymer from the aqueous reaction media. By removing excess of water in the polymer solution, the surface resistance was observed to reduce from 6 MΩ/□ to 16 KΩ/□.

Secondary doping step was performed on the polyaniline doped with DBSA in order to reduce the surface resistance of the polymer thin film further. *p*-TSA, *m*-cresol and thymol were three counter anions that were used using solution and film doping techniques to apply the secondary doping. Due to the unique structure of *p*-TSA, the surface resistance was found to reduce from 16 KΩ/□ to 0.65 KΩ/□ that are remarkable.

As a conclusion, introducing an electron withdrawing group to the polymer backbone led to improve the solubility. Changing the intermolecular spacing between the polymer chains by using bulky counter anion also helpful to improve the solubility of the polymer. Secondary doping was a good approach for improving the electrical properties of polymer.

5.2 Future Work:

The poor electrical properties and lack of solubility are the two major limitations for the ICPs in order to be utilize the ICPs in the energy devices. The main focus of future work should be placed on manipulating the polymer performance in energy devices including polymer solar

cells, battery, supercapacitors and biosensors along with continuous efforts for enhancing the basic properties.

REFERENCES

1. Janardhan, V.; Fesmire, B. Energy Explained. Volume 1 Conventional Energy. **2011**.
2. Goldenberg, J. Energy What Everyone Needs to Know. **2012**.
3. Krupp, F.; Horn, M. The Race to Reinvent Energy and Stop Global Worming. Earth: The Sequel. **2008**.
4. http://www.eia.gov/todayinenergy/detail.php?id=26252
5. Kannan, N.; Vakeesan, D. Solar energy for future world: A review. Renew. *Sustain. Energy Rev*. **2016**, *62*, 1092– 1105.
6. Sengupta, D. Dasa, B.; Mondal, B.; Mukherjee, K. Effects of Doping, Morphology and Film-Thickness of Photo-Anode Materials for Dye Sensitized Solar Cell Application. Renew. Sustain. *Energy Rev*. **2016**, *60*, 356–376.
7. Mat Desa, M. K.; Sapeai, S.; Azhari, A. W.; Sopian, K.; Sulaiman, M. Y.; Amin, N.; Zaidi, S. H. Silicon back contact solar cell configuration: A pathway towards higher efficiency. *Renew Sustain Energy Rev*. **2016**, *60*, 1516–1532.
8. https://irenanewsroom.org/2016/04/10/renewable-energy-breaks-growth-record-in-2015/
9. Sperling, L. H. Introduction to physical polymer science. Fourth edition. **2006**.
10. Rodriguez, F. Principle of polymer systems. Third edition. **1989**.
11. MacDiarmid, A. G. “Synthetic Metals” A novel role for organic polymers. *Angew. Chem. Int. Ed*. **2001**, *40 (14)*, 2581-2590.
12. Gerard, M.; Chaubey, A.; Malhotra, B. D. Application of conducting polymers to biosensors. *Biosens. Bioelectric*. **2002**, *17(5)*, 345-359.

13. Kaur, G.; Adhikari, R.; Cass, P.; Bown, M.; Gunatillake, P. Electrically conductive polymers and composites for biomedical applications. *RSC Adv.* **2015**, *5(47)*, 37553-37567.

14. Facchetti, A. Facchetti, A. π-Conjugated Polymers for Organic Electronics and Photovoltaic Cell Applications. *Chem. Mater*. **2011**, *23(3)*, 733–758.

15. Kumar, D.; Sharma, R. C. Advance in conductive polymers. *Eur. Polym. J*. **1998**, *34(8)*, 1053-1060.

16. Moliton, A.; Hiorns, R. C. Review of electronic and optical properties of semiconducting π-conjugated polymers: application in optoelectronics. *Polym. Int*. **2004**, *53(10)*, 1397-1412.

17. Zhang, X.; Chen, L.; Wang, G.; Zhang, Z. G.; Li, Y.; Shen, P. Synthesis and photovoltaic properties of alkylthiothienyl-substituted benzo(1,2-b:4,5-b') dithiophene D-A copolymers with different accepting units. *Synthetic Metals*. **2016**, *211*, 121-131.

18. Shin, N.; Yun, H. J.; Yoon, Y.; Son, H. J.; Ju, S. Y.; Kwon, S. K.; Kim, B.; Kim, Y. H. Highly stable polymer solar cells based on poly(dithienobenzodithiophene-co-thienothiophene). *Macromolecules*. **2015**, *48(12)*, 3890-3899.

19. Hu, H.; Jiang, K.; Yang, G.; Liu, J.; Li, Z.; Lin, H.; Liu, Y.; Zhao, J.; Zhang, J.; Huang, F.; Qu, Y.; Ma, W.; Yan, H. Terthiophene-based D-A polymer with an asymmetric arrangement of alkyl chain that enables efficient polymer solar cells. *J. Am. Chem. Soc.* **2015**, *137(44)*, 14149-14157.

20. Elayappan, V.; Murugadoss, V.; Angaiah, S.; Fei, Z.; Dyson, P. D. Development of a conjugated polyaniline incorporated electrospun poly (vinylidene fluoride-co-hexafuoropropylene) composite membrane electrolyte for high performance dye-sensitized solar cells. *J. Appl. Polym. Sci*. **2015**, *132(45)*, 42777.

21. Kawabata, K.; Saito, M.; Osaka, I.; Takimiya, K. Very small bandgap π□conjugated polymers with extended thienoquinoids. *J. Am. Chem. Soc*. **2016**, *138(24)*, 7725−7732.

22. Zhou, N.; Dudnik, A. S.; Li, T. I. N. G.; Manley, E. F.; Aldrich, T. J.; Guo, P.; Liao, H. C.; Chen, Z.; Chen, L. X.; Chang, R. P. H.; Facchetti, A.; Cruz, M. O.; Marks, T. J. All-polymer solar cell performance optimized via systematic molecular weight tuning of both donor and acceptor polymers. *J. Am. Chem. Soc*. **2016**, *138(4)*, 1240−1251.

23. Melkonyan, F. S.; Zhao, W.; Drees, M.; Eastham, N. D.; Leonardi, M. J.; Butler, M. R.; Chen, Z.; Yu, X.; Chang, R. P. H.; Ratner, M. A.; Facchetti, A. F.; Marks, T. J. Bithiophenesulfonamide Building Block for π□Conjugated Donor− Acceptor Semiconductors. *J. Am. Chem. Soc*. **2016**, *138(22)*, 6944−6947.

24. Held, M.; Zakharko, Y.; Wang, M.; Jakubka, F.; Gannott, F.; Rumer, J. W.; Ashraf, R. S.; McCulloch, I.; Zaumseil, J. Photo- and electroluminescence of ambipolar, high-mobility, donor-acceptor polymers. *Organic Electronics*. **2016**, *32*, 220-227.

25. Wang, N.; Chen, Z.; Wei, W.; Jiang, Z. Fluorinated benzothiadiazole-based conjugated polymers for high-performance polymer solar cells without any processing additives or post treatments. *J. Am. Chem. Soc*. **2013**, *135(45)*, 17060-17068.

26. Yuan, L.; Zhao, Y.; Zhang, J.; Zhang, Y.; Zhu, L.; Lu, K.; Yan, W. Oligomeric donor material for high-effeciency organic solar cells: breaking down a polymer. *Adv. Mater*. **2015**, *27(28),* 4229–4233.

27. Wang, T.; Wang, H.; Li, G.; Li, M.; Bo, Z.; Chen, Y. Thiophene-fused 1,10-phenanthroline and its conjugated polymers. *Macromolecules.* **2016**, *49(11)*, 4088-4094.

28. Li, Y.; Zou, J.; Yip, H. L.; Li, C. Z.; Zhang, Y.; Chueh, C. C.; Intemann, J.; Xu, Y.; Liang, P. W.; Chen, Y.; Jen, A. K. Y. Side-chain effect on Cyclopentadithiophene/ fluorobenzothiadiazole-based low band gap polymers and their applications for polymer solar cells. *Macromolecules*. **2013**, *46(14)*, 4597-5503.

29. Rochat, S.; Swager, T. M. Water-soluble cationic conjugated polymers: response to electron-rich bioanalyte. *J. Am. Chem. Soc*. **2013**, *135(47)*, 17703-17706.

30. Corbet, J. P.; Mignani, G. Selected cross-coupling reaction technologies. *Chem. Rev*. **2006**, *106(7)*, 2651-2710.

31. Carsten, B.; He, F.; Son, H. J.; Xu, T.; Yu, L. Stille polycondensation for synthesis of functional materials. *Chem. Rev*. **2001**, *111(3)*, 1493-1527.

32. Thompson, B.; Kim, Y. G.; McCarley, T. D.; Reynolds, J. Soluble narrow band gap and blue propylenedioxythiophene- cyanovinylene polymers as multifunctional materials for photovoltaic and electrochromic applications. *J. Am. Chen. Soc*. **2006**, *128(39)*, 12714-12725.

33. Li, G.; Zhu, R.; Yang, Y. Polymer solar cells. *Nature. Photon*. **2012**, *6(3)*, 153-161.

34. Liang, Y.; Xu, Z.; Xia, J.; Tsai, S. T.; Wu, Y.; Li, G.; Ray, C.; Yu, L. For the bright future-bulk heterojunction polymer solar cells with power conversion efficiency of 7.4%. *Adv. Mater*. **2010**, *22(20)*, E135-E138.

35. Coakley, K. M.; McGehee, M. D. Conjugated polymer photovoltaic cells. *Chem. Mater*. **2004**, *16(23)*, 4533-4542.

36. Chen, C. W., Hermle, M., Benick, J., Tao, Y., Ok, Y. W., Upadhyaya, A., ... & Rohatgi, A. Modeling the potential of screen printed front junction CZ silicon solar cell with tunnel oxide passivated back contact. *Prog. Photovolt.* **2017**, *25(1),* 49-57.

37. Jeong, S.; Garnett, E. C.; Wang, S.; Yu, Z.; Fan, S.; Brongersma, M. L.; McGehee, M. D.; Cui, Y. Hybrid Silicon Nanocone−Polymer Solar Cells. *Nano Lett*. **2012**, *12*, 2971−2976.

38. Li, W.; Furlan, A.; Hendriks, K. H.; Wienk, M. M.; Janssen, R. A. J. Efficient tandem and triple-junction polymer solar cells. *J. Am. Chem. Soc*. **2013**, *135(15)*, 5529-5532.

39. An, Q.; Zhang, F.; Li, L.; Wang, J.; Sun, Q.; Zhang, J.; Tang, W.; Deng, Z. Simultaneous Improvement in Short Circuit Current, Open Circuit Voltage, and Fill Factor of Polymer Solar Cells through Ternary Strategy. *ACS Appl. Mater. Interfaces* **2015**, *7(6)*, 3691−3698.

40. Guo, X.; Zhou, n.; Lou, S.;Smith, J.;Tice D. B.;Hennek, H. W.; Ortize, R. P.; Navarrete, J. T. L.; Li, S.; Strzalka, J.; Chen, L. X.; Chang, R. P. H.;Facchetti, A.; Marks, T. J. Polymer solar cells with enhanced fill factors. *Nature Photon*. **2013**, *7(6)*, 825-833.

41. Zhou, H.; Zhang, Y.; Seifter, J.; Collins, S. D.; Luo, C.; Bazan, G. C.; Nguyen, T. Q.; Heeger, A. J. High-efficiency polymer solar cells enhanced by solvent treatment. *Adv. Mater.* **2013**, *25(11)*, 1646–1652.

42. Chen, C. C.; Chang, W. H.; Yoshimura, K.; Ohya, K.; You, J.; Gao, J.; Hong, Z.; Yang, Y. An efficient triple-junction polymer solar cells having a power conversion efficient exceeding 11%. *Adv. Mater*. **2014**, *26(32)*, 5670-5677.

43. Liu, D.; Yang, J.; Kelly, T. L. Compact layer free perovskite solar cells with 13.5% efficiency. *J. Am. Chem. Soc*. **2014**, *136(49)*, 17116−17122.

44. Im, J. H.; Luo, J.; Franckevičius, M.; Pellet, N.; Gao, P.; Moehl, T.; Zakeeruddin, S. M.; Nazeeruddin, M. K.; Grätzel, M.; Park, N. G. Nanowire Perovskite Solar Cell. *Nano Lett*. **2015**, *15(3)*, 2120−2126.

45. Conway, B. E. Electrochemical Supercapacitors: Scientific Fundamentals and technological applications. **2013**.

46. Faraji, S.; Ani, F. N. The development supercapacitor from activated carbon by electroless plating. Renewable and Sustainable Energy Reviews. 2015, 42, 823–834.

47. Snook, G. A.; Kao, P.; Best, A. S. Conducting-polymer-based supercapacitor devices and electrodes. *J. Power Sources*. **2011**, *196(1)*, 1-12.

48. Forse, A. C.; Merlet, C.; Griffin, J. M.; Grey, C. P. New perspectives on the charging mechanisms of supercapacitors. *J. Am. Chem. Soc*. **2016**, *138(18)*, 5731−5744.

49. Suga, T.; Ohshiro, H.; Sugita, S.; Oyaizu, K.; Nishide, H. Emerging N-type redox-active radical polymer for a total organic polymer based rechargeable battery. *Adv. Mater.* **2009**, *21(16)*, 1627-1630.

50. Wang, S.; Gai, L.; Zhou, J.; Jiang, H.; Sun, Y.; Zhang, H. Thermal cyclodebromination of polybromopyrroles to polymer with high performance for supercapacitor. *J. Phy. Chem. C.* **2015**, *119(8)*, 3881-3891.

51. Kim, T. Y.; Jung, G.; Yoo, S.;Suh, K. S.; Ruoff, R. S. Activated graphene-based carbons as supercapacitor electrodes with macro- and mesopores. *Acs. Nano*. 2013, *7(8),* 6899-6905.

52. Wang, Z.; Carlsson, D. O.; Tammela, P.; Huo, K.; Nyholm, L.; Stomme, M. Surface modified nanocellulose fobers yield conducting polymer-based flexible supercapacitors with enhanced capacitances. *Acs. Nano*. **2015**, *9(7)*, 7563–7571.

53. Estrada, L. A.; Liu, D. Y.; Salazar, D. H.; Dyer, A. L.; Reynolds, J. R. Poly [bis-EDOT-isoindigo]: an electroactive polymer applied to electrochemical supercapacitors. *Macromolecules*. **2012**, *45(20)*, 8211-8220.

54. McQuade, D. T.; Pullen, A. E.; Swager, T. M. Conjugated polymer-based chemical sensors. *Chem. Rev.* 2000, *100(7),* 2537-2574.

55. Feng, X.; Cheng, H.; Pan, Y.; Zheng, H. Development of glucose biosensors based on nanostructured graphene-conducting polyaniline composite. *Biosens. Bioelectric*. **2015**, *70*, 411-417.

56. Li, L.; Wang, Y.; Pan, L.; Shi, Y.; Cheng, W.; Shi, Y.; Yu, G. A nanostructured conductive hydrogels-based biosensor platform for human metabolite detection. *Nano Lett*. **2015**, *15(2)*, 1146−1151.

57. Zeng, W.; Yang, X.; Chen, X.; Yan, Y.; Lu, X.; Qu, J.; Liu, R. Conjugated polymers containing 2-thiohydantoin: Detection of cuprous ion, hydrogen peroxide and glucose. *European Polymer Journal*. **2014**, *61*, 309–315.

58. Melo, J. S. D.; Takato, S.; Sousa, M.; Melo, M. J.; Parola, A. J. Revisiting Perkin's dye(s): the spectroscopy and photophysics of two new mauveine compounds (B2 and C). *Chem. Commun*. **2007**, *(25)*, 2624–2626.

59. MacDiarmid, A. G., Chiang, J. C., Richter, A. F., Somasiri, N. L. D., & Epstein, A. J. Polyaniline: synthesis and characterization of the emeraldine oxidation state by elemental analysis. In *Conducting polymers*. **1987**, 105-120. Springer Netherlands.

60. Chiang, J. C., & MacDiarmid, A. G. 'Polyaniline': Protonic acid doping of the emeraldine form to the metallic regime. *Synth. Met*. **1986,** *13*(1-3), 193- 205.

61. MacDiarmid, A. G., Chiang, J. C., Huang, W., Humphrey, B. D., & Somasiri, N. L. D. Polyaniline: protonic acid doping to the metallic regime. *Mol. Cryst. Liq. Cryst.* **1985**, *125*(1), 309-318.

62. MacDiarmid, A. G.; Epstein, A. J. Secondary doping: a new concept in conducting polymers. *Macromol. Symp*. **1995**, *98(1)*, 835-842.

63. Matveeva, E. S. Could the acid doping of polyaniline represent the charge transfer interaction? *Synth. Met*. **1996**, *83(2)*, 89-96.

64. Parkhutik, V. P.; Matveeva, E. S. Effect of molecular doping by hydroquinones on morphology and optical properties of polyaniline. *J. Am. Chem. Soc*. **1998**, *102(9)*, 1549-1555.

65. Fu, Y.; Elsenbaumer, R. L. Thermochemistry and kinetics of chemical polymerization of aniline determined by solution calorimetry. *Chem. Mater.* **1994**, *6(5)*, 671-677.

66. Bhadra, S.; Kim, N. H.; Lee, J. H. Synthesis of water soluble sulfonated polyaniline and determination of crystal structure. *Applied Polymer Science*. 2010, *117(4)*, *2025*- 2035.

67. Sapurina, I.; Tenkovtsevb, A. V.; Stejskala, J. Conjugated polyaniline as a result of the benzidine rearrangement. *Polym. Int.* **2015**, *64(4)*, 453–465.

68. Kinlen, P. J.; Liu, J; Ding, Y.; Graham, C. R.; Remsen, E. E. Emulsion Polymerization Process for Organically Soluble and Electrically Conducting Polyaniline. *Macromolecules*. **1998**, *31(6)*, 1735-1744.

69. Kinlen, P. J.; Frushour, B. G.; Ding, Y.; Menon, V. Synthesis and characterization of organically soluble polyaniline and polyaniline block copolymers. *Synth. Met*. 1999, *101(1-3),* 758-761.

70. Lee, K. S.; Hino, T.; Kuramoto, N. Highly conductive polyaniline doped with DEHSSA synthesize in different protonic acid. *Chemistry Letters*. **2007**, *36(2)*, 340-341.

71. Erdem, E.; Karakıs, M. Sacak, M. The chemical synthesis of conductive polyaniline doped with dicarboxylic acids. *European Polymer Journal*. **2004**, *40(4)*, 785–791.

72. Bhadra, S., Khastgir, D., Singha, N. K., & Lee, J. H. Progress in preparation, processing and applications of polyaniline. *Progress in polymer science*. **2009**, *34*(8), 783-810.

73. Li, G. R., Feng, Z. P., Zhong, J. H., Wang, Z. L., & Tong, Y. X. Electrochemical synthesis of polyaniline nanobelts with predominant electrochemical performances. *Macromolecules*. **2010**, *43*(5), 2178-2183.

74. Wang, Y., Jing, X., & Kong, J. Polyaniline nanofibers prepared with hydrogen peroxide as oxidant. *Synth. Met*. **2007**, *157*(6), 269-275.

75. Surwade, S. P., Agnihotra, S. R., Dua, V., Manohar, N., Jain, S., Ammu, S., & Manohar, S. K. Catalyst-free synthesis of oligoanilines and polyaniline nanofibers using H_2O_2. *J. Am. Chem. Soc.* **2009**, *131*(35), 12528-12529.

76. Matveeva, E. S. Residual water as a factor influencing the electrical properties of polyaniline. The role of hydrogen bonding of the polymer with solvent molecules in the formation of a conductive polymeric network. *Synth. Met.* **1996**, *79*(2), 127-139.

77. Zhao, W., Ye, L., Zhang, S., Fan, B., Sun, M., Hou, J. Ultrathin polyaniline-based buffer layer for highly efficient polymer solar cells with wide applicability. *Scientific reports*. **2013**, *4*, 6570-6570.

78. Abdulrazzaq, O., Bourdo, S. E., Woo, M., Saini, V., Berry, B. C., Ghosh, A., Biris, A. S. Comparative Aging Study of Organic Solar Cells Utilizing Polyaniline and PEDOT: PSS as Hole Transport Layers. *ACS Applied Materials & Interfaces*. **2015**, *7(50)*, 27667-27675.

79. Geethalakshmi, D., Muthukumarasamy, N., Balasundaraprabhu, R. CSA-doped PANI/TiO 2 hybrid BHJ solar cells–Material synthesize and device fabrication. *Materials Science in Semiconductor Processing*. **2016**, *51*, 71-80.

80. Mohsennia, M., Bidgoli, M. M., Khoddami, M. H., Salehi, A., & Boroumand, F. A. Bulk-heterojunction polymer solar cells with polyaniline-silica nanocomposites as an efficient hole-collecting layer. *Journal of Nanophotonics*. **2016**, *10*(1), 016011-016011.

81. Li, X.; Zhang, C.; Xin, S.; Yang, Z.; Li, Y.; Zhang, D.; Yao, P. Facile synthesis of MoS2/reduced graphene oxide @polyaniline for high-performance supercapacitors. *ACS Appl. Mater. Interfaces.* **2016**, *8(33)*, 21373−21380.

82. Moussa, M.; El-Kady, M. F.; Zhao, Z.; Majewski, P.; Ma, J. Recent progress and performance evaluation for polyaniline/graphene nanocomposites as supercapacitor electrodes. *Nanotechnology*, **2016**, *27(44)*, 442001-442022.

83. Wang, G.; Zhang, Y.; Zhou, F.; Sun, Huang, F.; Yu, Y.; Chen, L.; Pan, M. Simple and fast synthesis of polyaniline nanofibers/ carbon paper composites as supercapacitor electrodes. Journal of energy storage. **2016**, *7*, 99-103.

84. Ge, D., Yang, L., Fan, L., Zhang, C., Xiao, X., Gogotsi, Y., Yang, S. Foldable supercapacitors from triple networks of macroporous cellulose fibers, single-walled carbon nanotubes and polyaniline nanoribbons. *Nano Energy*. **2015**, *11*, 568-578.

85. Liu, Y., Ma, Y., Guang, S., Ke, F., Xu, H. Polyaniline-graphene composites with a three-dimensional array-based nanostructure for high-performance supercapacitors. *Carbon*. **2015**, *83*,79-89.

86. Zhang, J., Wang, J., Yang, J., Wang, Y., Chan-Park, M. B. Three-dimensional macroporous graphene foam filled with mesoporous polyaniline network for high areal capacitance. *ACS Sustainable Chemistry & Engineering*. **2014**, *2(10)*, 2291-2296.

87. Yu, P., Li, Y., Zhao, X., Wu, L., Zhang, Q. Graphene-wrapped polyaniline nanowire arrays on nitrogen-doped carbon fabric as novel flexible hybrid electrode materials for high-performance supercapacitor. *Langmuir*. **2014**, *30(18)*, 5306-5313.

88. Mitchell, E., Candler, J., De Souza, F., Gupta, R. K., Gupta, B. K., Dong, L. F. High performance supercapacitor based on multilayer of polyaniline and graphene oxide. *Synth. Met*. **2015**, *199*, 214-218.

89. Tran, V. C.; Nguyen, V. H.; Nguyen, T. T.; Lee, J. H.; Huynh, D. C.; Shim, J. J. Polyaniline and multi-walled carbon nanotube-intercalated graphene aerogel and its electrochemical properties. *Synth. Met*. **2016**, *215*, 150-157.

90. Wang, L., Feng, X., Ren, L., Piao, Q., Zhong, J., Wang, Y., Wang, B. Flexible solid-state supercapacitor based on a metal–organic framework interwoven by electrochemically-deposited PANI. *J. Am. Chem. Soc.* 2015, *137(15)*, 4920-4923.

91. Kumar, J., Shahabuddin, M., Singh, A., Singh, S. P., Saini, P., Dhawan, S. K., & Gupta, V. (2015). Highly sensitive chemo-resistive ammonia sensor based on dodecyl benzene sulfonic acid doped polyaniline thin film. *Sci. Adv. Mater.* ***2015***, 7(3), 518-525.

92. Kumar, V.; Patil, V.; Apte, A.; Harale, N.; Patil, P.; Kulkarni, S. Ultrasensitive Gold Nanostar−Polyaniline Composite for Ammonia Gas Sensing. *Langmuir* **2015**, *31(48)*, 13247−13256.

93. Radhakrishnan, S.; Krishnamoorthy, K.; Sekar, C.; Wilson, J.; Kim, S. J. A promising electrochemical sensing platform based on ternary composite of polyaniline–Fe_2O_3–reduced graphene oxide for sensitive hydroquinone determination. *Chem. Engine. J.* **2015**, *259*, 594–602.

94. Zhu, J.; Huo, X.; Liu, X.; Ju, H. Gold nanoparticles deposited polyaniline-TiO_2 nanotube for surface plasmonic resonance enhanced photoelectrochemical biosensors. *ACS Appl. Mater. Interfaces*. **2016**, *8(1)*, 341-349.

95. Cihaner, A., & Önal, A. M. Synthesis and characterization of fluorine-substituted polyanilines. *European polymer journal.* **2001**, *37*(9), 1767-1772.

96. Ito, S., Murata, K., Teshima, S., Aizawa, R., Asako, Y., Takahashi, K., & Hoffman, B. M. Simple synthesis of water-soluble conducting polyaniline. *Synth. Met*. **1998**, *96*(2), 161-163.

97. Krebs, F. C. Fabrication and processing of polymer solar cells: a review of printing and coating techniques. *Solar energy materials and solar cells*. **2009**, *93*(4), 394-412.

98. Maenosono, S., Okubo, T., & Yamaguchi, Y. Overview of nanoparticle array formation by wet coating. *Journal of Nanoparticle Research*. **2003**, *5*(1-2), 5-15.

99. Mohseni, E., Zalnezhad, E., & Bushroa, A. R. Comparative investigation on the adhesion of hydroxyapatite coating on Ti–6Al–4V implant: A review paper. *Inter. J. Adhes. Adhes*. **2014**, *48*, 238-257.